ELSEVIER

Coordination Chemistry Reviews 143 (1995)
331–381

COORDINATION CHEMISTRY REVIEWS

Cluster-stabilized cations: syntheses, structures, molecular dynamics and reactivity

Michael J. McGlinchey*, Luc Girard, Ralph Ruffolo

Department of Chemistry, McMaster University, Hamilton, Ont. L8S 4M1, Canada

Received 26 August 1994; in revised form 22 December 1994

Contents

* Corresponding author.

SSDI 0010-8545(95)01131-5

Abstract

Tetrahedral clusters possessing two or three organometallic vertices, such as $Co(CO)_3$ or $CpMo(CO)_2$, provide enormously enhanced stability to neighboring cationic centers. The factors controlling the interactions between the electron-deficient centers and the metals are discussed in terms of their frontier molecular orbitals. Rational syntheses of these systems are now available, and many such metal-stabilized cations have been isolated and characterized not only spectroscopically but also by X-ray crystallography. These species exhibit a variety of fluxional processes which have been elucidated by variable-temperature nuclear magnetic resonance (NMR) measurements and also by a Bürgi–Dunitz analysis of a series of closely related X-ray crystal structures. By preparing clusters containing different organometallic fragments, it is possible to establish a hierarchy of moieties best able to alleviate the electron deficiency at the carbenium ion center. Finally, the growing usage of these metal-stabilized carbocations in organic synthesis, in the elucidation of reaction mechanisms and even in biological chemistry is described.

Keywords: Cluster-stabilized cations; Syntheses; Structure; Molecular dynamics; Reactivity

1. Introduction

The ability of neighboring atoms to provide anchimeric assistance to electron-deficient centers is well established in conventional organic chemistry. Typically, the rate of hydrolysis of 2,2'-dichlorodiethyl sulfide (**1**) (the mustard gas of World War I) is enormously enhanced compared with that found for ordinary primary alkyl halides. This occurs because the neighboring sulfur atom can provide a lone pair of

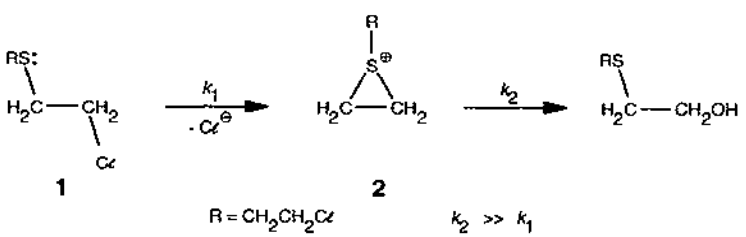

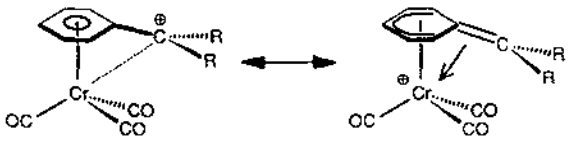

3

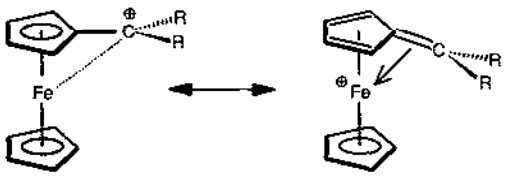

4

electrons to alleviate the developing cationic charge on carbon; rapid nucleophilic attack on the sulfonium ion intermediate (**2**) leads to product formation [1].

Analogously, a wide variety of organometallic moieties, such as ferrocenyl [2], (cyclobutadienyl)Fe(CO)$_3$ [3], (cyclobutadienyl)Co(C_5H_5) [4] and (cyclopentadienyl)Cr(CO)$_2$NO [5], have been shown to provide neighboring group assistance to developing cationic centers; this pioneering work has been reviewed previously [6]. Typically, the 100,000-fold rate enhancement in benzyl halides, when π complexed to Cr(CO)$_3$, has been attributed to stabilization of the intermediate cation by interaction with the electron-rich metal center [7]. Indeed, in recent years, these proposed benzyl cationic intermediates, such as **3**, have been characterized by nuclear magnetic resonance (NMR) spectroscopy [8–11]. Even more convincingly, the structure of the ferrocenylmethyl cation (**4**) has been determined by X-ray crystallography [12,13], and the 22° bend of the sp^2-hybridized carbocationic center towards the metal atom has been rationalized in terms of a fulvene ligand coordinated to a (C_5H_5)Fe$^+$ moiety [14].

In the light of these observations, it is perhaps not unexpected that metal clusters, which can be viewed as three-dimensionally aromatic with a highly polarizable electron cloud [15–17], should be capable of alleviating the positive charge on proximally attached atoms or molecular fragments. Indeed, the capacity of metal clusters for cation stabilization is almost unsurpassed, and in this paper we describe the syntheses, structures, molecular dynamics and reactivity of such species.

2. Cations derived from tricobalt nonacarbonyl carbyne complexes

2.1. Synthetic aspects

The original route to carbynyltricobaltnonacarbonyl clusters ($Co_3(CO)_9CR$) was serendipitous; protonation of the known complex (HC≡CH)Co$_2$(CO)$_6$ with concentrated H_2SO_4 led to $Co_3(CO)_9C-CH_3$, which was characterized crystallographically

[18]. Subsequently, a more convenient, general synthesis was developed; this method involved the reaction of $Co_2(CO)_8$ with a range of trichloromethyl-containing reagents, and led to a wide variety of tetrahedral tricobalt clusters [19]. The first rational preparation of a cluster cation was reported by Seyferth and coworkers [20] at the Massachusetts Institute of Technology (MIT), who found that protonation of the cluster carboxylic acid, $Co_3(CO)_9C–CO_2H$, or the corresponding ester, $Co_3(CO)_9C–CO_2R$, led to the acyl cation $[Co_3(CO)_9C–C{=}O]^+$ (**5**). Furthermore, it was shown that the use of HPF_6 as the protonating agent gave an isolable salt which could be weighed, conveniently stored and used in further reactions when needed. Seyferth and coworkers noted that **5** was a sterically protected acylium salt, entirely analogous to those encountered during the acid-catalyzed hydrolysis of aromatic esters bearing bulky ortho substituents, as in **6** [21].

It was also noted that the treatment of $Co_3(CO)_9CBr$ with $AlCl_3$ followed by quenching with a nucleophile, such as methanol, gave the methyl ester **7** rather than

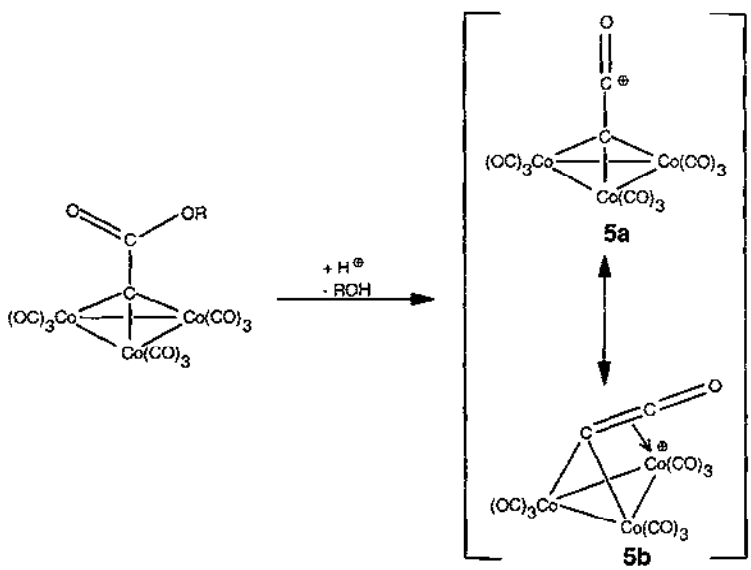

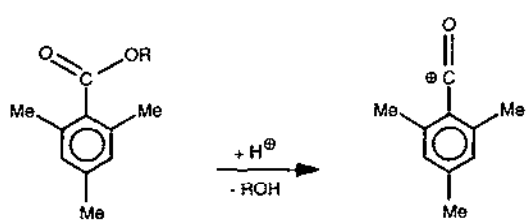

6

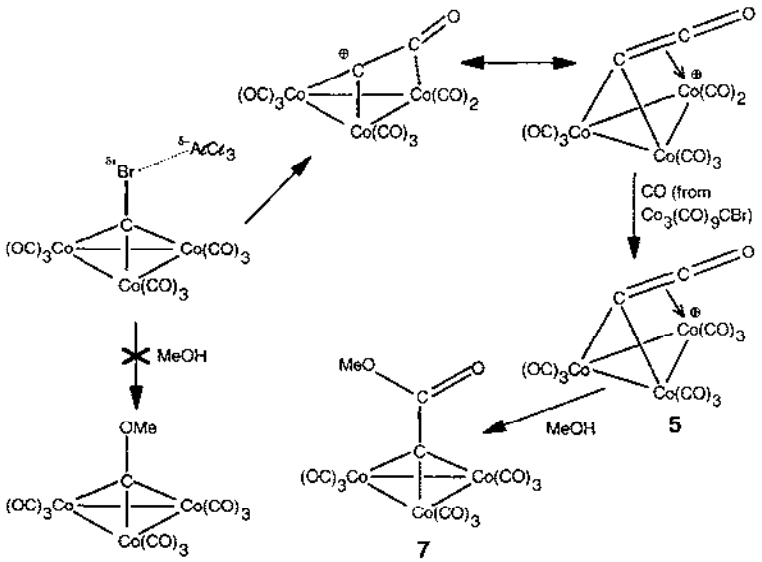

Scheme 1. Proposed mechanism for the formation of $[Co_3(CO)_9C{-}C{\equiv}O]^+$ (**5**) from $Co_3(CO)_9CBr$ and a Lewis acid.

the methyl ether, again suggesting the intermediacy of the acylium ion **5** [22,23]. The proposed mechanism is shown in Scheme 1.

Concurrently, the MIT group were also investigating the effect of protonating cluster alcohols or ethers, such as **8**, which again led to cluster-stabilized cations **9** [23]. With typical insight, Seyferth suggested that the remarkable ease of formation of these alkyl and acyl cations arose as the result of a stabilizing interaction of the cationic carbon with a cobalt vertex. As noted previously, such a rationale has been invoked to account for the enhanced reactivity of monometallic species, such as ferrocenylmethanol, and of $Cr(CO)_3$-complexed benzyl halides.

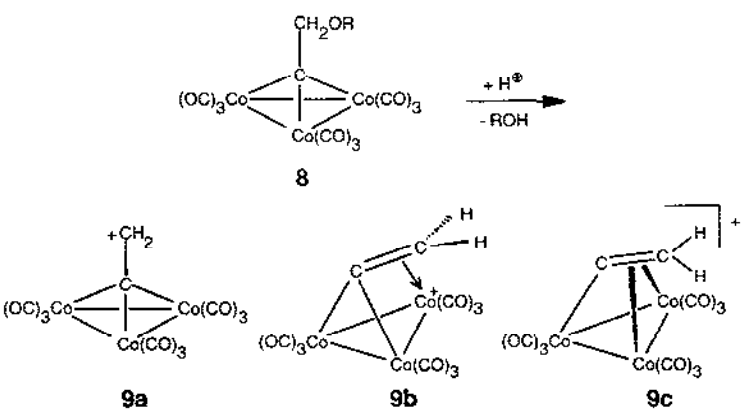

2.2. Molecular orbital calculations

Our understanding of the bonding in these cluster cations derives principally from extended Hückel molecular orbital (EHMO) calculations carried out initially by Schilling and Hoffmann [24]. In a now classic paper, they described the interactions of the frontier orbitals of triangular M_3L_9 fragments with a variety of capping groups. The orbital pattern of an $Fe_3(CO)_9$ triangle can be constructed from suitable symmetry-adapted combinations of the three constituent $Fe(CO)_3$ moieties [25].

As shown in Fig. 1, each $M(CO)_3$ fragment contributes three frontier orbitals to the triangular unit. The lowest of these is primarily d_{xy} hybridized towards the missing sites of the octahedron from which the fragment was formally derived. These three in-plane orbitals yield a doubly degenerate 1e set and a high-lying a_2 orbital. The former are filled and provide good metal–metal bonding interactions, while the latter (which is an entirely out-of-phase combination) is also in the plane of the metals but is normally vacant. The combination of d_z^2 orbitals from the three constituent $M(CO)_3$ fragments produces the classic a_1 π-type orbital as well as the doubly degenerate π^* set of e symmetry; this orbital level pattern is analogous to that of the π manifolds found in cyclopropenium and related systems. It is noteworthy, however, that these d_z^2 combinations do not overlap well with orbitals of the capping group which are aligned along the C_3 axis of the cluster. However, this role is more than adequately filled by the in-phase combination of the remaining orbitals of the

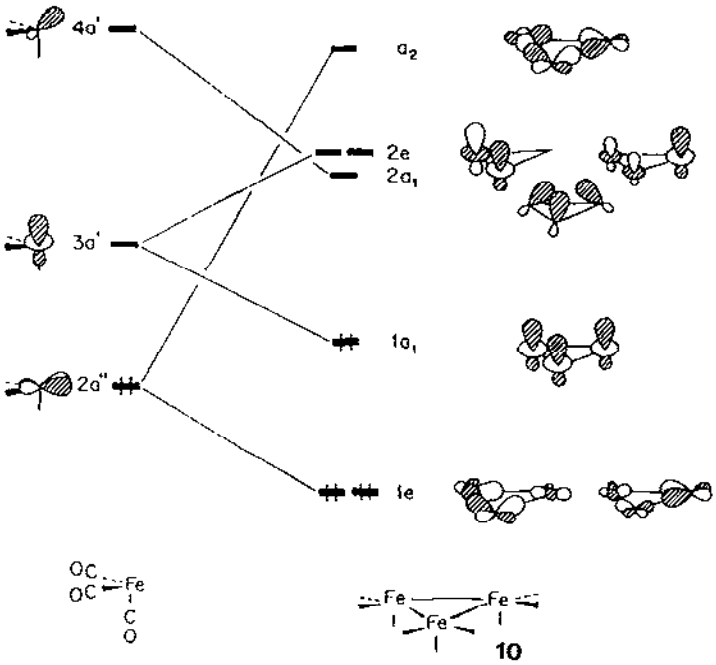

Fig. 1. Interaction of three $Fe(CO)_3$ units to form $Fe_3(CO)_9$ (adapted from Ref. [24]).

$M(CO)_3$ fragment; each of these is a mixture of s, p_z and d_{z^2} and their bonding combination is oriented perfectly to interact with the capping atom [24].

To summarize therefore, metal triangles such as $[Fe_3(CO)_9]$ (**10**) or $[Co_3(CO)_9]^{3+}$ (**11**) give rise to a low-lying set of three filled orbitals ($1e+1a_1$) and, at somewhat higher energy, a set of three vacant orbitals ($2a_1+2e$) which serve to accept electron density from capping ligands. In the light of the EHMO analysis presented above, it is apparent that a carbyne moiety (represented formally as HC^{3-}) has a filled sp-hybridized orbital ideally oriented to interact with the vacant $2a_1$ combination of the $[Co_3(CO)_9]^{3+}$ triangle. Moreover, the two occupied π orbitals of the carbyne have the correct symmetry to overlap with the degenerate 2e acceptor pair, as shown in Fig. 2.

Schilling and Hoffmann [24] extended these concepts to the cluster carbocations prepared by Seyferth and coworkers. In particular, they examined the conformations available to the alkyl cation $[Co_3(CO)_9C{=}CH_2]^+$ (**9**). They were able to show that the linear cation **9a** is actually an energy maximum, with essentially no barrier to rotation of the CH_2 group relative to the basal plane. Moreover, the minimum energy structure **9b**, in which the vinylidene cap bends towards a cobalt atom, is stabilized because of a very favorable interaction between the symmetrical component of the 2e set of the metal triangle and the π orbital of the $C{=}CH_2$ unit. This latter orbital is well localized on the methylene carbon and creates direct bonding between

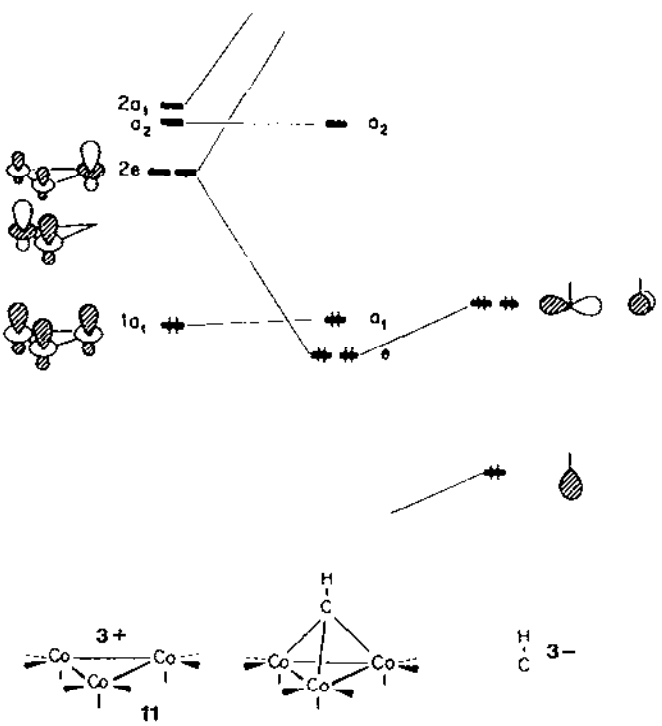

Fig. 2. Interaction diagram for $Co_3(CO)_9CH$ (adapted from Ref. [24]).

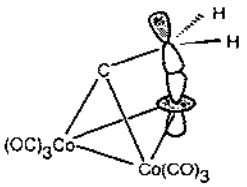

Fig. 3. The interaction of a vacant p_z orbital on the cationic carbon with a filled d_{z^2} orbital on cobalt.

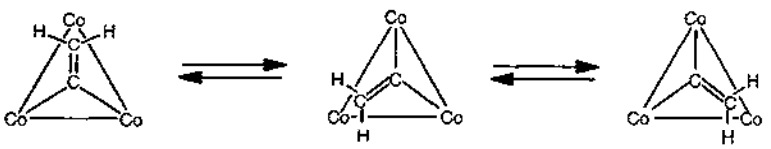

Fig. 4. Migration of the vinylidene fragment around the metal triangle in $[Co_3(CO)_9C{=}CH_2]^-$ (**9**).

this carbon and a cobalt atom (see Fig. 3); as a result, the gap between the highest occupied molecular orbital (HOMO) and the lowest unoccupied molecular orbital (LUMO) increases markedly on bending the $C{=}CH_2$ moiety towards a $Co(CO)_3$ vertex.

Schilling and Hoffmann [24] also noted that, when the vinylidene cap is oriented towards a cobalt–cobalt vector, as in **9c**, there is a somewhat weaker interaction of the methylene p_z orbital with the antisymmetric component of the 2e set of the tricobalt fragment. In this conformation, the methylene hydrogens are oriented in an upright manner relative to the basal plane. Since molecule **9c** lies about 16 kcal mol^{-1} above the favored structure **9b**, it represents a saddle point in the antarafacial migration process which allows the vinylidene cap to bond to each cobalt center successively, as in Fig. 4.

2.3. Structures of ketenylidene and vinylidene complexes

Although no X-ray crystallographic data on the prototypical cations **5** or **9** have yet been reported, the structures of these tricobalt species may be inferred not only from spectroscopic evidence, but also from solid state data on closely analogous molecules. The structural chemistry of ketenylidenes complexed to iron cluster frameworks has been largely pioneered by Shriver and coworkers [26–30], who prepared the anions $[Fe_3(CO)_9C{=}C{=}O]^{2-}$ and $[Fe_2Co(CO)_9C{=}C{=}O]^-$ (**12** and **13** respectively). In the Fe_3 cluster **12**, the ketenylidene moiety is not aligned along the C_3 axis of the iron triangle, but rather is tilted 33° towards one of the $Fe(CO)_3$ vertices [26]; in the Fe_2Co anion **13**, this angle θ is 24° [27]. Interestingly, in the congeneric ruthenium cluster $[Ru_3(CO)_9C{=}C{=}O]^{2-}$ (**14**), the $C{=}C{=}O$ unit leans through 11° towards an Ru–Ru vector [28]. Continuing down the group, Shapley et al. [31] have prepared the dianion $[Os_3(CO)_9C{=}C{=}O]^{2-}$ (**15**), which exhibits an angle θ of 26°; however, in the corresponding diprotonated species $H_2Os_3(CO)_9C{=}C{=}O$,

in which the extra two hydrogens are bonded to the Os atoms in the basal plane, the ketenylidene unit is almost perpendicular to the tri-osmium plane [31].

EHMO calculations on these ketenylidene systems reveal orbital interactions which are closely analogous to those previously discussed for the vinylidene-capped trimetallic clusters. In particular, these calculations show that the capping C=C=O fragment can be stabilized by leaning towards either a metal vertex or a metal–metal bond, as shown in Fig. 5 [32]. In the tricobalt system $[Co_3(CO)_9C\ C{=}O]^+$ (**5**), the HOMO–LUMO gap is already substantial even in the C_{3v} structure **5a**, but it does improve as the ketenylidene leans towards a cobalt vertex, as in **5b**. However, the effect is less dramatic than in the corresponding vinylidene cationic cluster **9b**.

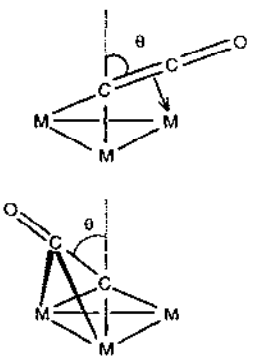

12 $[Fe_3(CO)_9C{=}C{=}O]^{2-}$, θ = 33°

13 $[Fe_2Co(CO)_9C{=}C{=}O]^{1-}$, θ = 24°

15 $[Os_3(CO)_9C{=}C{=}O]^{2-}$, θ = 26°

14 $[Ru_3(CO)_9C{=}C{=}O]^{2-}$, θ = 11°

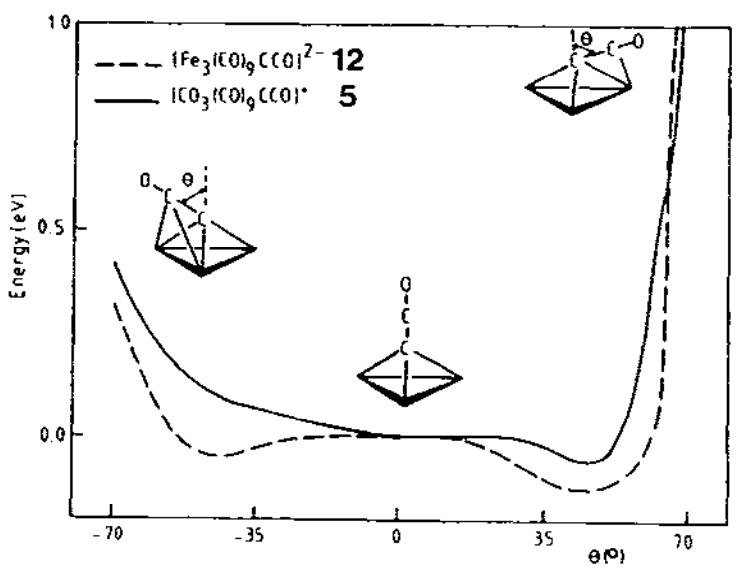

Fig. 5. Energy level diagram showing the effect of tilting the capping ketenylidene unit from the threefold axis perpendicular to the plane of the metals in $[Co_3(CO)_9C{-}C{-}O]^+$ (**5**) and $[Fe_3(CO)_9C{=}C{-}O]^{2-}$ (**12**).

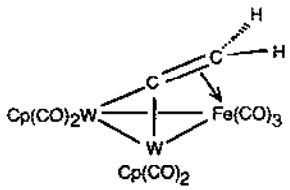

16

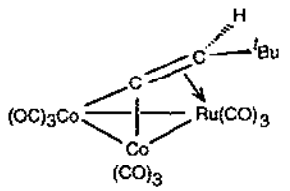

17

For $[Fe_3(CO)_9C{=}C{=}O]^{2-}$ (**12**), the calculations reveal two shallow minima, of which the lower (depth, approximately 3 kcal mol^{-1}) corresponds to a tilting of the capping group through about 40° towards an iron vertex. As noted above, the crystallographic data show a bend of 33° in this direction. The capping ketenylidene in the ruthenium analogue **14** tilts the other way, i.e. towards a ruthenium–ruthenium vector, perhaps corresponding to the other minimum on the graph shown in Fig. 5.

Although no X-ray crystallographic structure determinations of $[Co_3(CO)_9C{=}CR_2]^+$ clusters have yet been reported, data have been obtained for neutral clusters which have the same overall electron count. In $(C_5H_5)_2W_2(CO)_4Fe(CO)_3C{=}CH_2$ (**16**) and $Co_2(CO)_6Ru(CO)_3C{=}CH^tBu$ (**17**), the vinylidene leans towards the $Fe(CO)_3$ or $Ru(CO)_3$ vertex respectively [33,34]. Thus we can formally assign an 18 electron configuration to all three metal atoms in each cluster.

2.4. NMR studies on vinylidene cations

The EHMO calculations of Schilling and Hoffmann [24] suggest not only that the CH_2^+ group in $[Co_3(CO)_9C{=}CH_2]^+$ (**9**) will lean towards a $Co(CO)_3$ vertex, as in **9b**, but also that the capping fragment can undergo antarafacial migration from one metal to another. This prediction prompted Edidin et al. [35] to devise a most ingenious experimental test for the ground state geometry and for this fluxional process. To this end, they synthesized the cation **18**, in which an isopropyl substituent was incorporated as a ^{13}C NMR probe for chiral conformations. In this system, conformation **18a** would have C_1 symmetry and the methyls in the isopropyl group would be diastereotopic and thus exhibit two ^{13}C NMR resonances. At low temperature this behavior is indeed observed. Furthermore, as the temperature is raised, these two methyl peaks coalesce, as would be required for a pathway involving **18b**

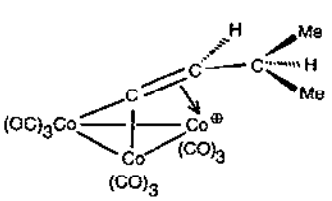

18a

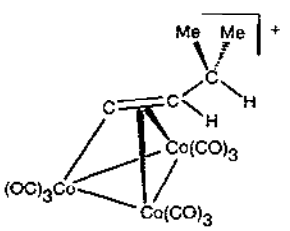

18b

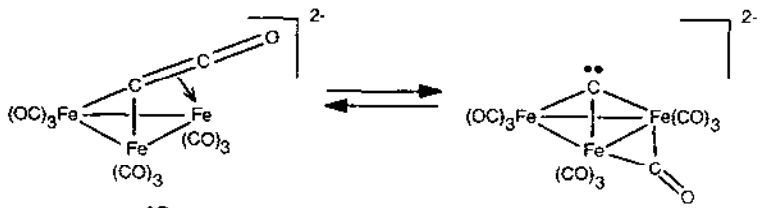

12a **12b**

which possesses a molecular mirror plane and so equilibrates the methyl environments. The experimentally determined barrier for this antarafacial migration process is 10.5 kcal mol^{-1}.

2.5. NMR studies on ketenylidene cations

Of course, in the case of the tricobalt ketenylidene cation $[Co_3(CO)_9C–C{=}O]^+$ (**5**), it is not possible to lower the symmetry of the capping acylium moiety and, in the absence of X-ray crystallographic data, we must resort to other techniques. It is noteworthy that at 163 K the ^{13}C NMR resonances of the cobalt carbonyls are split into a 6:3 ratio; this result has been rationalized in terms of the non-linear C_s structure **5b**, in which two rapidly rotating $Co(CO)_3$ vertices are different from the third [32]. In support of this view, we note that, in the closely analogous vinylidene complex $[Co_3(CO)_9C{=}CMe_2]^+$, the carbonyl resonances are likewise split into a 6:3 pattern at low temperature [36].

In Shriver's studies [26–30] of $[Fe_3(CO)_9C{=}C{=}O]^{2-}$ (**12**), it was observed that, when a sample of **12** was stirred overnight under an atmosphere of ^{13}CO, both the terminal and ketenylidene CO groups were enriched, as determined by ^{13}C NMR [26]. The enrichment of the apical carbonyl is thought to occur intramolecularly via the intermediate formation of a carbide **12b**; thus incorporation of ^{13}CO at the iron carbonyl positions provides a route to enrichment of the ketenylidene moiety. However, while this Fe–CO/C–CO interchange is operative only on the relatively slow chemical time scale, it is not detectable on the NMR time scale. Thus, even at 50 °C, the peaks attributable to the ketenylidene carbonyl and the CO groups bonded to iron show no evidence of exchange.

The corresponding ^{13}CO incorporation experiments were carried out on the tricobalt cation $[Co_3(CO)_9C–C{=}O]^+$ (**5**), but only the metal carbonyls were enriched [37]. However, the ketenylidene carbon in **5** has been labelled by treatment of ^{13}CO-enriched $Co_3(CO)_9CBr$ with $AlCl_3$, as in Scheme 1 [32].

3. $Co_2(CO)_6$- and $Cp_2Mo_2(CO)_4$-complexed propargyl cations

3.1. Syntheses and NMR fluxionality of dicobalt complexes

The ideas promulgated by Wade [15], Mingos [16] and Rudolph [38] have allowed a convenient classification of structural types, and have demonstrated the

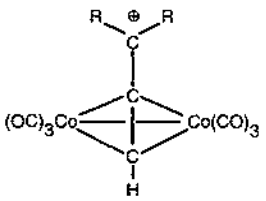

19a

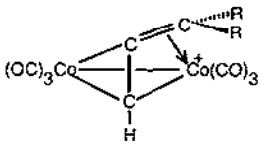

19b

relationships between molecular geometries and skeletal electron counts in clusters. Moreover, the concept of isolobality [39], whereby chemically different molecular fragments possess frontier orbitals of similar symmetry, energy, extension in space and electron occupancy, has provided a simple theoretical framework with which to rationalize much of cluster chemistry. We can replace a $Co(CO)_3$ vertex in $[Co_3(CO)_9C{=}CR_2]^+$ (**9**) by an isolobal CH fragment to generate the propargyl cation $[Co_2(CO)_6(HC{\equiv}C{-}CR_2)]^+$ (**19**); these molecules are readily available by protonation of alkynol complexes, such as $Co_2(CO)_6(HC{\equiv}C{-}CR_2OH)$ [40,41].

The bent structure **19b** was supported by NMR data, which revealed the non-equivalence of the methylene hydrogens, one of which would be syn with respect to the Co–Co vector, while the other would be anti relative to this bond [42]. The first mechanistically revealing study of such a system was reported by Schreiber et al. [43] who showed not only that the antarafacial migration process, **20**⇌**20′**, is valid for propargyl-dicobalt cations, but also that a second, and higher energy, fluxional process can be detected. This latter exchange is depicted in Scheme 2 and involves rotation about the C_α–C_β bond so as to interconvert the syn and anti hydrogen environments.

As with the tricobalt ketenylidene and vinylidene clusters (**5** and **9** respectively), it has not been possible to obtain X-ray quality crystals of the propargyl-dicobalt cations **19**. Nevertheless, isolobal substitution of a $Co(CO)_3^+$ vertex by an $Fe(CO)_3$ group should, in principle, yield a neutral cluster with the same electron count and, presumably, a similar structure. Indeed, EHMO calculations on the $(HC{\equiv}C{-}CH_2)FeCo(CO)_6$ cluster favor a structure in which the methylene moiety leans towards the $Fe(CO)_3$ vertex such that it makes an angle θ of approximately 55°. Very recently, this proposal has received experimental support and the cluster $(MeC{=}C{-}CH_2)FeCo(CO)_5PPh_3$ has been crystallographically characterized [44]. The structure is shown in Fig. 6 and the excellent correlation with the calculated geometry is evident; the experimental value of θ is 59°.

3.2. $Cp_2Mo_2(CO)_4$-stabilized monocations and dications

3.2.1. Syntheses

Concurrent with the work on alkyne-dicobalt complexes, Sokolov and his colleagues in Moscow were developing the chemistry of the analogous Group VI-stabilized cations $[Cp_2M_2(CO)_4(HC{\equiv}C{-}CR_2)]^+$ (**21**), where M ≡ Mo or W, either by using HBF_4–ether to protonate the precursor alcohols

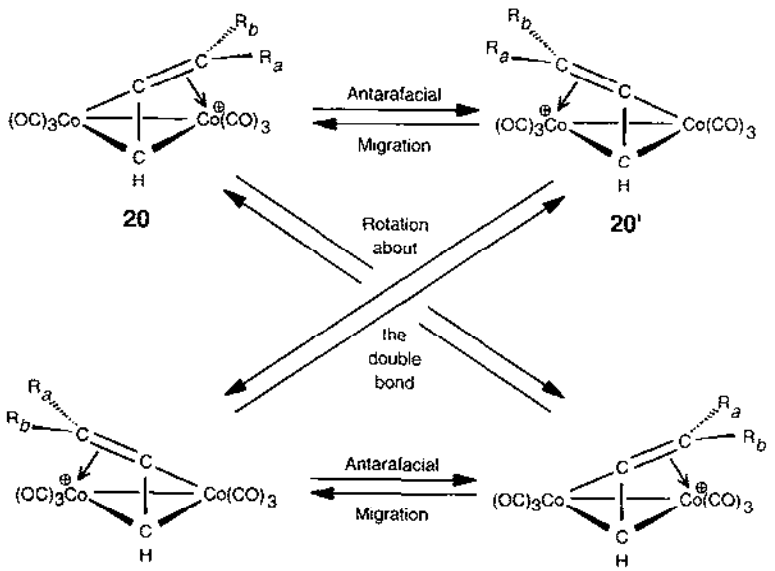

20 20'

Scheme 2. Fluxional processes in $[Co_2(CO)_6(HC{\equiv}C\text{-}CR_2)]^+$ (**20**).

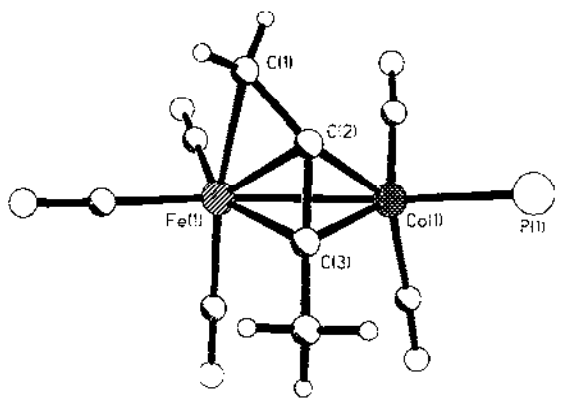

Fig. 6. X-Ray crystal structure of $(MeC{\equiv}C\text{-}CH_2)FeCo(CO)_5PPh_3$ showing how the methylene unit leans towards the $Fe(CO)_3$ vertex; phenyl groups have been removed for clarity.

$Cp_2Mo_2(CO)_4(RC{\equiv}C\text{–}CR_2OH)$, or by hydride abstraction from an allene precursor [45,46]. As shown in Scheme 3, molecules of this type are also accessible via protonation of the σ,η^2-allenylidene complexes $Cp_2M_2(CO)_4(\sigma,\eta^2\text{-}C{=}C{=}CMe_2$, where $M \equiv Mo$ or W [47]).

Sokolov and coworkers [48] also showed that the protonation of $Cp_2Mo_2(CO)_4(HOCH_2C{\equiv}C\text{–}CH_2OH)$ with HBF_4–ether afforded initially the monocation $[Cp_2Mo_2(CO)_4(HOCH_2C{\equiv}C\text{–}CH_2)]^+$ (**22**); subsequent treatment with FSO_3H or trifluoroacetic acid furnished the dication

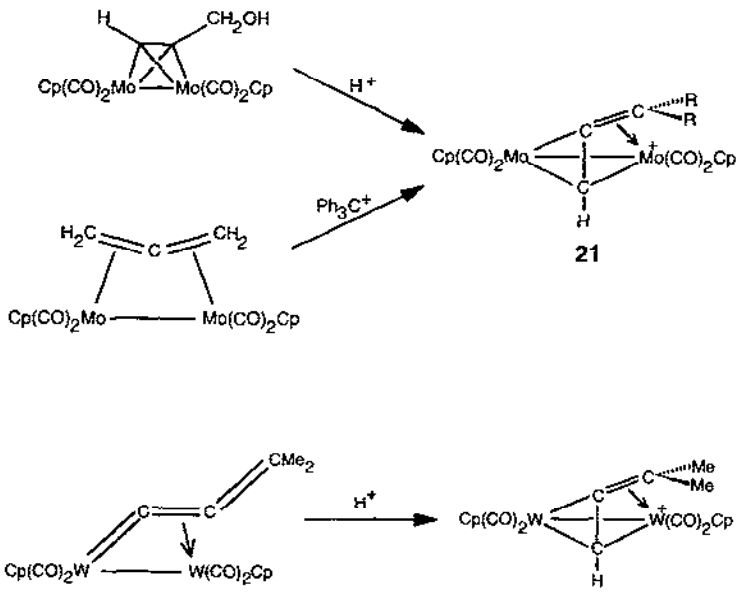

Scheme 3. Synthetic routes to the cationic clusters $[Cp_2M_2(CO)_4\{HC{\equiv}C{-}CR_2\}]^+$, where M ≡ Mo, W.

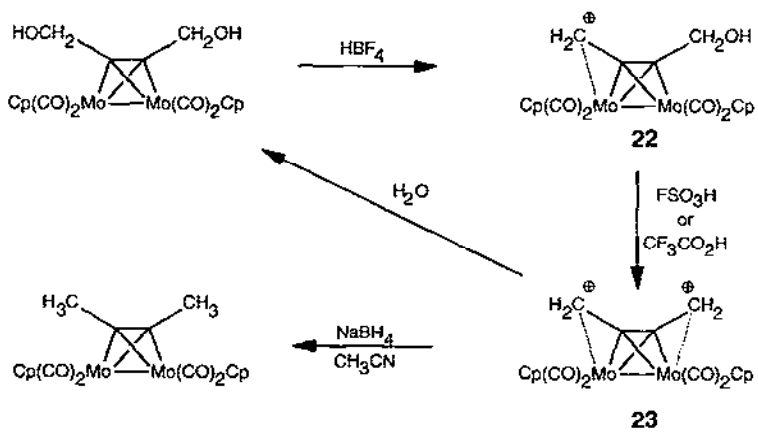

Scheme 4. Synthesis and reactivity of $[Cp_2Mo_2(CO)_4(H_2C{-}C{\equiv}C{-}CH_2)]^{2+}$ (**23**).

$[Cp_2Mo_2(CO)_4(CH_2C{\equiv}C{-}CH_2)]^{2+}$ (**23**). As illustrated in Scheme 4, the addition of water to **23** regenerated the starting but-2-yne-1,4-diol complex, whereas reduction of **23** with sodium borohydride gave $Cp_2Mo_2(CO)_4(CH_3C{\equiv}C{-}CH_3)$ [48].

3.2.2. NMR fluxionality

The original synthesis and characterization of tetrahedral clusters of the type $Cp_2Mo_2(CO)_4(RC{\equiv}CR)$ (**24**) were reported by Cotton and coworkers [49] who

noted a hitherto unknown feature in these structures. The molecules did not adopt a C_{2v} structure; instead the cyclopentadienyl rings were oriented in a less symmetrical manner. More interesting, however, was the arrangement of the carbonyls, three of which were almost linear, while the fourth CO ligand took up a semi-bridging position with an Mo=C=O angle in the range 165°–170°. The fluxional behavior of the $Cp_2Mo_2(CO)_4(RC{\equiv}CR)$ clusters also exhibited novel characteristics. A low energy process involved a pairwise exchange of the semi-bridging carbonyl with a terminal CO on the other molybdenum. A second process led to time-averaged C_{2v} symmetry via a swivelling motion of the two $CpMo(CO)_2$ vertices, as shown in Scheme 5.

These same structural features occur in $[Cp_2Mo_2(CO)_4(HC{\equiv}C{-}CR_2)]^+$ cations and, when the fluxional behavior is slow on the NMR time scale, this yields mixtures of diastereomers in which the semi-bridging carbonyls adopt different positions; the net result is a rather complex NMR spectrum at low temperature [50,51]. Nevertheless, it has been possible to delineate two exchange processes. The barrier to antarafacial migration of the CR_2^+ moiety from one molybdenum vertex to the other can be evaluated by monitoring the coalescence behavior of the cyclopentadienyl ring nuclei in either the ^1H or ^{13}C regimes. To be specific, the antarafacial migration process shown in Scheme 6 maintains the identity of the syn and anti substituents at C_β but equilibrates the metal sites. Interconversion of the syn and anti substituents requires rotation about the C_α–C_β bond.

These aspects are beautifully illustrated in the $[(C_5H_4Me)_2Mo_2(CO)_4(HC{\equiv}C{-}CH_2)]^+$ cation for which Curtis and coworkers [52] demonstrated that the cyclopentadienyl ligands are equilibrated via a process with an activation energy of about 17 kcal mol^{-1}; in contrast, the barrier for interconversion of the syn and anti CH_2 protons is considerably higher. These data are entirely in accord with the antarafacial migration and C_α–C_β rotation mechanisms depicted in Scheme 6.

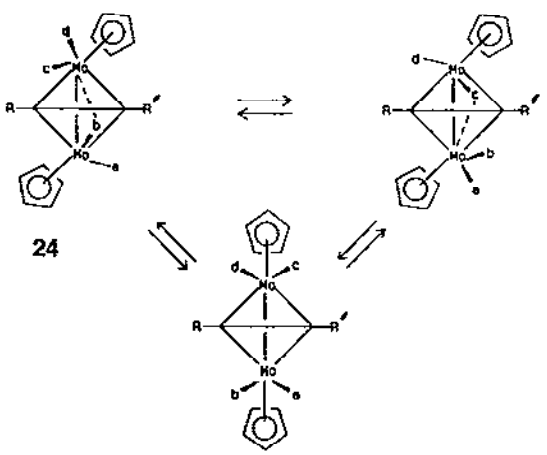

Scheme 5. Fluxional processes in $Cp_2Mo_2(CO)_4(RC{\equiv}CR)$ (**24**); initially, semi-bridging carbonyls are equilibrated, and subsequently the Cp groups become equivalent.

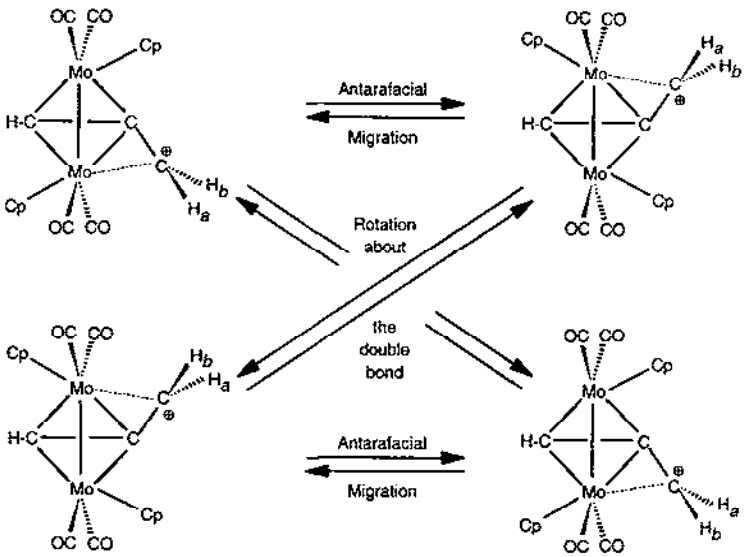

Scheme 6. Fluxional processes in $[Cp_2Mo_2(CO)_4(HC{\equiv}C{-}CH_2)]^+$ (21).

Subsequent investigations have revealed that the barrier to these antarafacial migrations of CR_2^+ fragments from one metal vertex to the other is critically dependent on the primary, secondary or tertiary character of the carbocationic center [47,50–55]. The activation energy for such a process in molybdenum-, tungsten- or cobalt-stabilized CR_2^+ moieties falls from approximately 18 kcal mol^{-1} for primary cations to about 10 kcal mol^{-1} for tertiary cations, indicating that the more stable tertiary centers have much less need for anchimeric assistance from the metal than primary cations. (These NMR data for metal-stabilized cations in solution have been complemented by variable-temperature cross-polarization magic angle spinning (CPMAS) studies in the solid state where the same processes are observed [51,55].)

Of particular significance are the data reported for the $[(fulvalene)Mo_2(CO)_4(RC{\equiv}C{-}CR_2)]^+$ cations (**25**) first described by Vollhardt and coworkers [53]. In these molecules, the cyclopentadienyl rings are linked and the carbonyl ligands are clearly terminally bonded. Naturally, these features restrict the mobility of the system and avoid the spectroscopic complications arising from the differing orientations of cyclopentadienyl rings and semi-bridging carbonyls [56]. Variable-temperature NMR and two-dimensional exchange studies on a number of these fulvalene systems allow us to determine a consistent pattern in their fluxional behavior. In $[\eta^5{:}\eta^5\text{-}(C_5H_4{-}C_5H_4)Mo_2(CO)_4(MeC{\equiv}C{-}CH_2)]^+$, the barrier towards antarafacial migration of the CH_2^+ moiety from Mo to Mo can be monitored by the rate of equilibration of the sets of fulvene ring protons; $\Delta G_{343}^{\ddagger}$ for this process was evaluated as approximately 17.7 kcal mol^{-1}. In contrast, the barrier to interconversion of the syn and anti methylene environments was found to be about 19.1 kcal mol^{-1}. A convenient way to express this result is that, at 343 K, there are approximately seven antarafacial migrations for each rotation about the $C{-}CH_2$ bond [53].

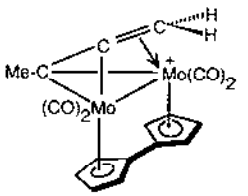

25

By way of contrast, in $[\eta^5{:}\eta^5\text{-}(C_5H_4{-}C_5H_4)Mo_2(CO)_4(HC{\equiv}C\text{-}CMe_2)]^+$, the antarafacial migration process and the barrier to rotation of the CMe_2 group are both approximately 10 kcal mol^{-1}. Similarly, in the diphenyl analogue $[(fulvalene)Mo_2(CO)_4(HC{\equiv}C{-}CPh_2)]^+$, both barriers are low [54].

4. X-Ray crystallography as a probe for the molecular dynamics of $[Cp_2Mo_2(CO)_4(propargyl)]^+$ cations

4.1. Structures of $[Cp_2Mo_2(CO)_4(RC{=}CR_2)]^+$ cluster cations

A major advantage of working with dimolybdenum cations, $[Cp_2Mo_2(CO)_4(RC{\equiv}C\text{-}CR'R'')]^+$, rather than their $Co_2(CO)_6$ analogues, **19**, is the ready availability of X-ray quality crystals of the former. A number of such cations have been characterized crystallographically, and in all cases the $(C{=}CR'R'')^+$ fragment leans towards a molybdenum vertex. However, the NMR evidence cited above suggests a reduced need for anchimeric assistance from the metal as the inherent stability of the carbocation ($CH_3^+ < RCH_2^+ < R_2CH^+ < R_3C^+$) increases [50–55]. This apparent weakening of the metal-to-carbocation interaction is also reflected in the increasing $Mo{-}C^+$ distances which range from 2.44 to 2.74 Å in the series $M{-}CH_2^+$, $M{-}CHR^+$, $M{-}CR_2^+$ [52–54,57–62]. However, these structural data do much more than merely yield the molecular geometry of the cations. They can also be used to investigate the molecular dynamics of these systems by means of a Bürgi–Dunitz trajectory analysis, and we take a brief detour to discuss the basis of this approach.

4.2. The Bürgi–Dunitz trajectory model

In recent years, the powerful concepts developed by Bürgi and Dunitz [63] have greatly increased our understanding of molecular dynamics. It has been demonstrated that a succession of static X-ray structures can provide information about the dynamics of a reaction. In their now classic studies, Bürgi et al. [64] showed, for example, that a series of crystal structures of systems containing both a nucleophile and an organic carbonyl group can be used to obtain the trajectory of approach of the two reagents. It is clear from these data not only that the nucleophile attacks along a line making an angle of approximately 105° to the C=O bond, but also

that the trigonal planar sp^2 carbon atom is gradually transformed into a tetrahedral center. The significance of these observations for mechanistic organic chemistry is profound, and it was soon exploited by Baldwin [65] to rationalize the favorable or unfavorable nature of many ring-closure processes.

Another beautiful result from Dunitz's laboratory [66] showed how the distribution of crystal structures of more than 60 $(C_6H_5)_3P$–X fragments in many different environments can be related to the "two-ring flip" mechanism by which these chiral propeller-like moieties can undergo racemization. In this process, all three phenyl rings do not rotate at the same rate nor in the same direction, and this phenomenon should be reflected in the crystallographic results which capture a series of snapshots of the Ph_3P fragment in different environments. This crystallographically derived picture of the stereoisomerization pathway is complemented by force field calculations and variable-temperature NMR data on related Ar_3CH systems, which also favor the "two-ring flip" mechanism [67–70].

The ideas of Bürgi and Dunitz have also been adopted by Crabtree and Lavin [71], who used a series of X-ray crystal structures to show that carbonyl migration between two metal atoms proceeds via a trajectory in which a linear terminal ligand goes through a series of increasingly bent semi-bridging structures to a symmetrically bridging situation.

The Bürgi–Dunitz approach can also be applied to the problem of finding the migration pathway of a CR_2^- moiety in $[Cp_2Mo_2(CO)_4(HC{\equiv}C{-}CR_2)]^+$, from one molybdenum vertex to the other, as depicted in Scheme 6. Moreover, these data can be conveniently compared with the minimum energy trajectory predicted by molecular orbital calculations.

4.3. EHMO calculations on Mo_2C_2 cluster cations

As noted above, the simplest model for the migration of a propargyl cation between two $CpMo(CO)_2$ centers is provided by the conformationally rigid fulvalene complex, $[\eta^5{:}\eta^5\text{-}(C_5H_4{-}C_5H_4)Mo_2(CO)_4(MeC{\equiv}C{-}CH_2)]^+$. Taking this framework as a model, the energy hypersurface has been calculated for migration of a $C{-}CH_2^+$ unit over the surface of an Mo_2C triangular base. The coordinates of the CH_2 unit are defined in terms of three angles θ, ϕ and ω, where θ measures the bending of the methylene unit towards the Mo–Mo bond (see Fig. 7). As the methylene group is allowed to swivel away from the molecular mirror plane which bisects the molybdenum–molybdenum bond, the dihedral angle ϕ opens up from 0° towards 70°, at which point the $C{-}CH_2$ bond eclipses the carbynyl-carbon–molybdenum vector. The third degree of freedom, the twist angle ω, defines the positions of the methylene hydrogens. When all three components of the CH_2 unit lie in the molecular mirror plane ($\phi = 0°$), the ω values are 0° for H_{endo} and 180° for H_{exo}. As the methylene fragment swivels towards Mo, we might anticipate that the values $\omega(H_{endo})$ and $\omega(H_{exo})$ would gradually evolve towards 90° and −90° respectively. Fig. 8 shows the resulting hypersurface, calculated at the extended Hückel level of approximation, in which the angles θ and ϕ were incremented in units of 5° and 2° respectively. At

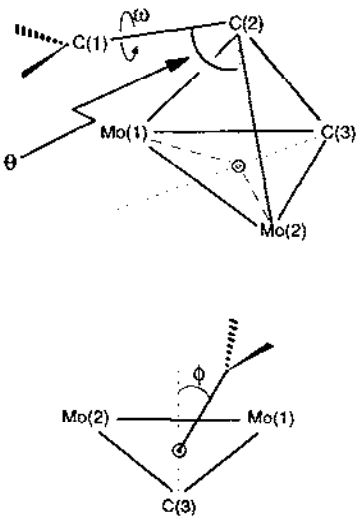

Fig. 7. The angles θ, ϕ and ω which define C(1) and C(2).

each point, the torsion angle ω was varied from 0° to 180° in 15° increments and the minimum energy ω value for each (θ,ϕ) position was plotted [72].

The transition state has C_s symmetry in which the optimal value of the bend angle θ is 175°, i.e. the CH_2 group leans only slightly towards the Mo–Mo vector. As ϕ increases to 20°, the initially relatively flat region of the hypersurface begins a precipitous drop into a potential well. This fall is accompanied by a sharp decrease in θ which becomes 140° by the time ϕ reaches 28°. The value of θ remains essentially constant as we approach the global minimum, and indeed is maintained briefly even after the C–CH_2 fragment has passed the $\phi = 70°$ mark, corresponding to the eclipsing of the carbynyl- carbon–molybdenum vector. The global minimum is located in the region $\phi = 50°–70°$, where the energy is virtually constant.

We can use these data to locate the minimum energy trajectory for this methylene migration process. Fig. 9 indicates the pathway taken by the methylene carbon, while Fig. 10 shows that, at $\phi = 0°$, the molecule maintains C_s symmetry such that the p_z orbital on the sp^2-hybridized CH_2^+ unit is oriented parallel to the Mo–Mo axis. This geometry optimizes the overlap of the vacant orbital of the cationic carbon with the filled d_z^2 orbitals on both metals and so stabilizes the electron-deficient methylene center during its transit from one molybdenum vertex to the other.

The orientation of the hydrogen atoms of the migrating group, as indicated by the torsional angle ω, was found to evolve with increasing ϕ so as to allow an optimal interaction of the carbon p orbital with the filled d orbital on the molybdenum atom towards which it is moving. Fig. 10 illustrates the evolution of the methylene twist angle ω as the migrating fragment seeks to maximize its orbital overlap with molybdenum as it approaches the metal center. Thus the plane containing the CH_2 fragment rotates relative to the Mo_2C basal triangle such that, when $\phi = 0°$, these two planes are orthogonal, but, at $\phi = 70°$, they are almost parallel.

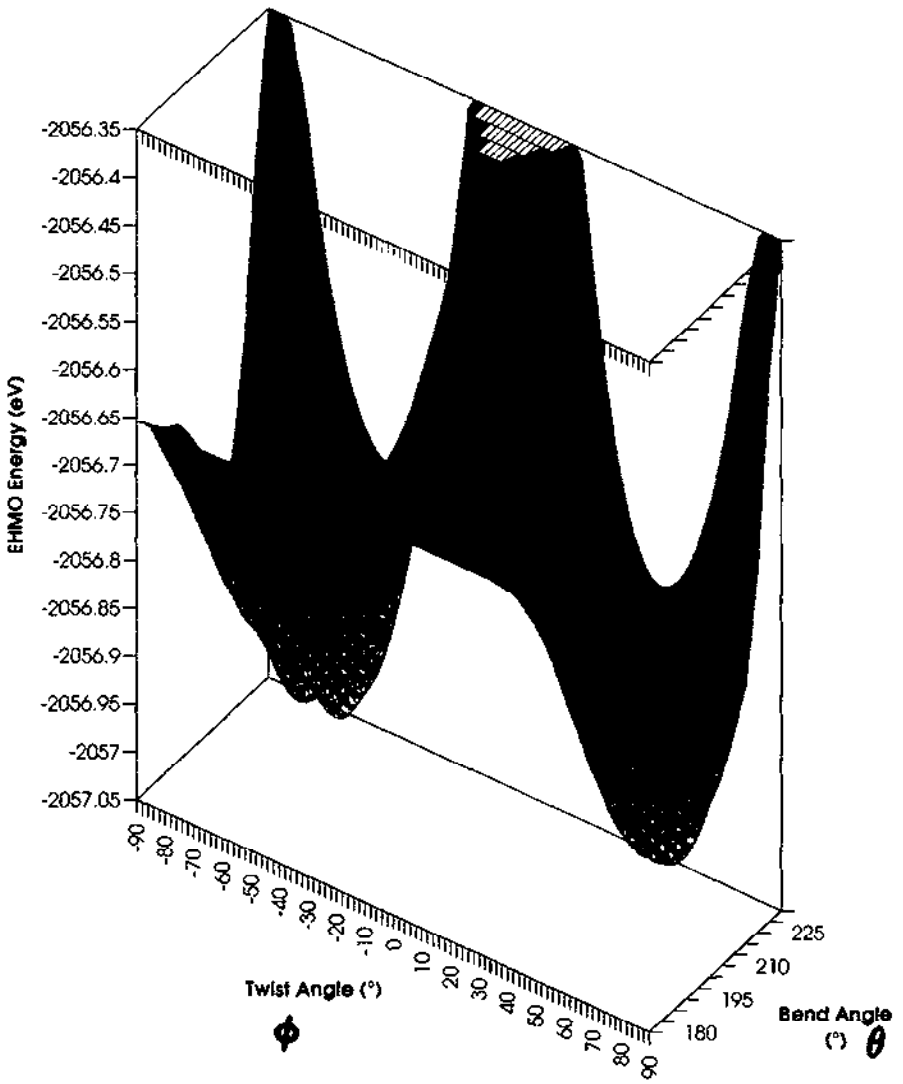

Fig. 8. EHMO-calculated hypersurface for the migration of a methylene group in $[(\eta^5;\eta^5$-fulvalene)$Mo_2(CO)_4(RC{\equiv}C{-}CH_2)]^+$ (**25**).

4.4. Comparison of EHMO-calculated structures with X-ray data for Mo_2C_2 cluster cations

In the light of these calculations, Girard et al. [72] assembled the available X-ray crystallographic data on the molybdenum cations, not only to carry out a Bürgi–Dunitz trajectory analysis, but also to complement their detailed EHMO investigation of the reaction pathway. Crystallographic data are available for a number of

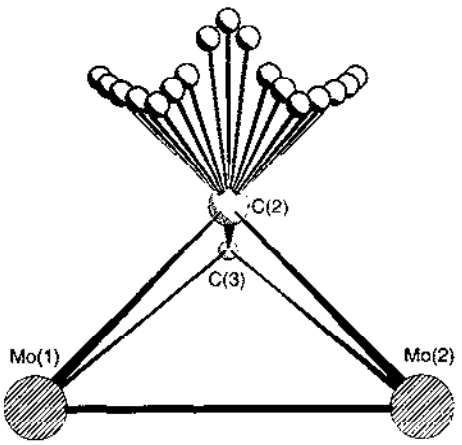

Fig. 9. View of the EHMO-calculated trajectory of C(1) during the antarafacial migration process.

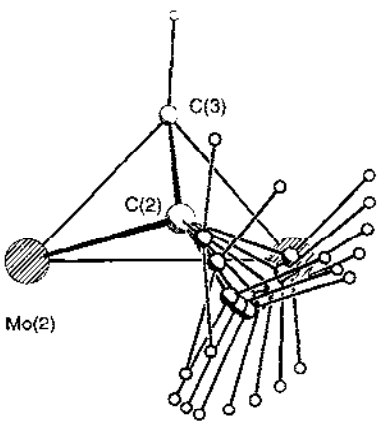

Fig. 10. Bird's eye view of the twisting motion of the CH_2 fragment during the antarafacial migration process.

$[Cp_2Mo_2(CO)_4(RC{\equiv}C{-}CR'R'')]^+$ cations, where Cp can be C_5H_5, C_5H_4Me or C_5Me_5, and the R′ and R″ substituents range from H [52,53,57], methyl [54,58] and ferrocenyl [59] to steroidal [60] and terpenoid [61,62] fragments; these data are summarized in Table 1.

As noted previously, the Mo–C^+ distances lengthen as the character of C^+ changes from a primary carbon, to a secondary carbon, and finally to a tertiary cationic center. However, for the present purpose, we need to know not only the bond distances, but also the experimental values of the bend angle θ and the torsional parameters ϕ and ω for each cationic cluster. Figs. 11 and 12 show the C–CH_2 positions for each of the 12 crystallographically determined structures which have been superimposed on the Mo_2C triangular base of $[\eta^5{:}\eta^5$-$(C_5H_4{-}C_5H_4)Mo_2(CO)_4(MeC{\equiv}C{-}CH_2)]^+$.

Table 1
Crystallographic data for molybdenum cations

Structure	r (Mo(1)−C(1)) (Å)	r (⊙−C(2)) (Å)	C(3)−⊙−C(2) (°)	r (C(2)−C(1)) (Å)	θ (⊙−C(2)−C(1)) (°)	ϕ (C(3)−⊙−C(2)−C(1)) (°)	Reference
$[(C_5H_4-C_5H_4)Mo_2(CO)_4(MeC{\equiv}C-CH_2)]^+$	2.442	1.248	71.3	1.475	123	61	[53]
$[(C_5H_5)_2Mo_2(CO)_4(HC{\equiv}C-CH_2)]^+$	2.444	2.315	68.3	1.379	122	58	[57]
$[(C_5H_4Me)_2Mo_2(CO)_4(HC{\equiv}C-CH_2)]^+$	2.465	1.358	67.0	1.345	124	53	[52]
$[(C_5H_4Me)_2Mo_2(CO)_4(HC{\equiv}C-CH_2)]^+$	2.468	1.324	69.0	1.437	122	53	[52]
$[(C_5H_4-C_5H_4)Mo_2(CO)_4(MeC{\equiv}C-CH_2)]^+$	2.557	1.251	70.9	1.484	128	51	[53]
$[(C_5H_5)_2Mo_2(CO)_4(HC{\equiv}C-CHMe)]^+$	2.613	1.354	70.7	1.380	132	72	[58]
$[(C_5H_5)_2Mo_2(CO)_4(BuC{\equiv}C-CH(\text{ferrocenyl}))]^+$	2.630	1.316	68.4	1.424	123	54	[59]
$[(C_5H_5)_2Mo_2(CO)_4(MeC{\equiv}C-\text{bornyl})]^+$	2.737	1.350	65.1	1.397	136	50	[61]
$[(C_5H_5)_2Mo_2(CO)_4(HC{\equiv}C-\text{mestranyl})]^+$	2.738	1.368	66.5	1.364	127	53	[60]
$[(C_5H_4-C_5H_4)Mo_2(CO)_4(HC{\equiv}C-CMe_2)]^+$	2.753	1.404	68.7	1.361	126	71	[54]
$[(C_5H_5)Mo(CO)_2Co(CO)_3(MeC{\equiv}C-\text{bornyl})]^+$	2.915	1.350	65.1	1.397	146	50	[61]
$[(C_5H_5)Mo(CO)_2Co(CO)_3(MeC{\equiv}C-\text{fenchyl})]^+$	3.079	1.351	69.4	1.366	155	52	[62]

⊙ is the centroid of the Mo_2C_2 tetrahedral cluster, as shown in Fig. 7.

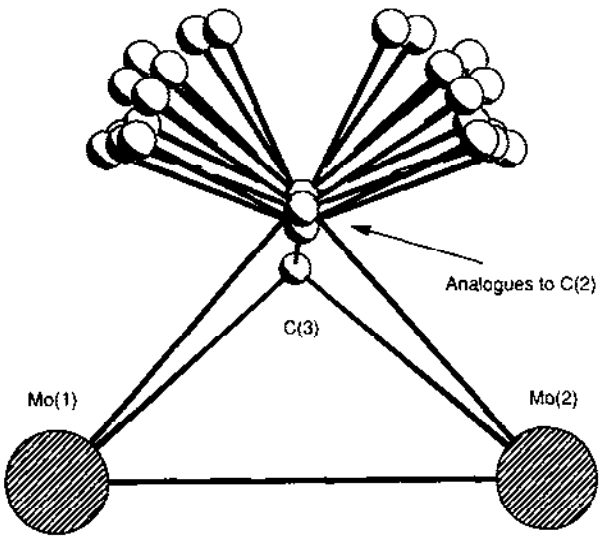

Fig. 11. Superposition of the C(1) cationic centers in 12 different X-ray crystal structures, $[Cp_2Mo_2(CO)_4(RC{\equiv}C{-}CR'R'')]^+$.

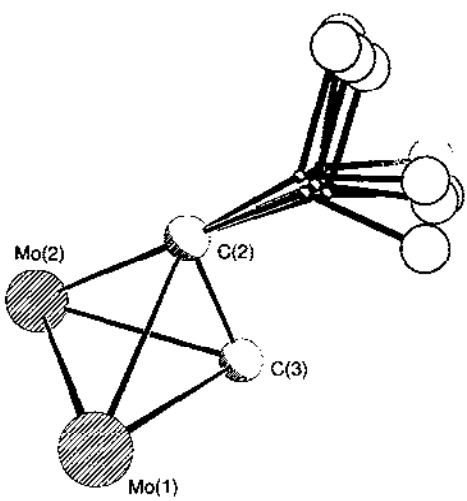

Fig. 12. View of the twisting motion of the CR'R'' fragment in a series of X-ray crystal structures.

It is immediately apparent from a comparison of Figs. 9 and 10 with Figs. 11 and 12 respectively that there is an excellent correlation between the EHMO-calculated and X-ray-determined series of structures. The crystallographically located positions of the carbynyl capping carbons in the series of clusters, although very similar, are not identical, showing that we can consider that the whole vinylidene fragment is

capable of moving over the triangular base. Nevertheless, it is evident that the locus of the cationic site is readily defined in terms of the angles θ and ϕ.

It is fortunate that the $[Cp_2Mo_2(CO)_4(RC{\equiv}C{-}CR'R'')]^+$ clusters whose structures have been reported cover a range of substituents with widely differing electronic and steric requirements, and so yield a data set with bend angles θ varying from 122° to 155° and with torsional angles ϕ covering the range 50°–70°. These values encompass almost the entire domain of the deep potential well in the hypersurface depicted in Fig. 8. Indeed, we can clearly see that the tertiary cationic centers have not merely lengthened the $Mo{-}C^+$ distances relative to those found in CH_2^- systems, but have also started to climb out of the potential well by rotating the $C{-}CH_2$ vector towards the mirror plane which bisects the two molybdenum vertices. Moreover, the twist angles ω gradually evolve such that the exo and endo substituents move towards their predicted vertical positions as the migration proceeds. We also note that, in those crystal structures where the substituents attached to C_β are observable, the cationic center is not planar in an ideal sp^2 fashion, but rather shows a tendency to pyramidalize. Of course, in those cases where the greatest pyramidalization is to be expected, i.e. the primary cations most firmly bonded to the metal center, the methylene hydrogens cannot be located unequivocally. Interestingly, the EHMO calculations suggest that, at the calculated global minimum energy for $[\eta^5{:}\eta^5\text{-}(C_5H_4{-}C_5H_4)Mo_2(CO)_4(HC{\equiv}C{-}CH_{\{2\}})]^+$ (where $\theta = 140°$ and $\phi = 54°$), the methylene hydrogens can each be bent away from the Mo atom by 8°; this stabilizes the system to the tune of approximately 1.2 kcal mol^{-1} [72].

In summary, the remarkable similarity between the calculated lowest energy pathway for cation migration between two metal vertices and the trajectory indicated by a series of crystallographic "snapshots" of the process is manifest evidence of the power of the Bürgi–Dunitz approach towards understanding molecular dynamics [73].

5. Reactivity of $[Co_3(CO)_9C{-}C{=}O]^+$ cluster cations

The acylium-type character of **5** and its isolobally related clusters **26–29**, whereby a $Co(CO)_3$ vertex has been replaced by a $(C_5H_5)Ni$, $(C_5H_5)Mo(CO)_2$, $(C_5Me_5)Mo(CO)_2$ or $(C_5H_5)Co(\mu\text{-}CO)$ moiety, should be reflected in the ease of reaction with nucleophiles.

Such is indeed the case, and these clusters have been treated with a wide variety of reagents [37,74,75]. Typically, alcohols, amines and thiols react to give the corresponding esters, amides and thioesters. The $[Co_3(CO)_9C{-}C{=}O]^+$ acylium ion can also be used in Friedel–Crafts acylations of electron-rich aromatic systems [74]. Thus **5** reacts with anisole, dimethylaniline or ferrocene to give the corresponding acyl clusters, as illustrated in Scheme 7; in contrast, the mixed-metal acylium clusters **26–28** are unreactive towards ferrocene, but do acylate pyrrole or indole.

It is informative to compare these results with those found for the corresponding anions, such as $[Fe_3(CO)_9C{=}C{=}O]^{2-}$ (**10**), which might naively have been expected to react analogously with electrophiles; however, the situation is not quite so simple.

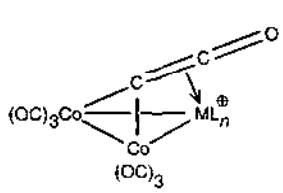

5 $ML_n = Co(CO)_3$

26 $ML_n = CpNi$

27 $ML_n = (C_5H_5)Mo(CO)_2$

28 $ML_n = (C_5Me_5)Mo(CO)_2$

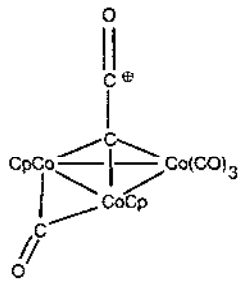

29

Under certain conditions, these anionic ketenylidenes (**30a**) behave as if they were in equilibrium with a trimetallic carbide form (**30b**). Indeed, Lavigne [76] has described these ketenylidene clusters in terms of a capping carbide atom being (lightly) stabilized by a carbonyl group. Thus small electrophiles, such as H^+ or CH_3^+, attack the α-carbon and the carbonyl moiety of the ketenylidene migrates to the metal triangle to give the alkylated cluster **31** [26]. In contrast, as shown in Scheme 8, an acetyl group bonds to the ketenylidene oxygen atom, **32**; subsequent protonation yields initially the closo cluster **33** and ultimately the isomer **34** in which the C_α–C_β bond has been cleaved [77].

It is noteworthy that the ruthenium cluster **14** differs not only structurally from its iron and osmium congeners **12** and **15**, but also in its chemical behavior. Electrophilic attack by H^+ or CH_3^+ occurs at a metal center rather than at the C=C=O capping fragment. This may be a consequence of the smaller value of θ

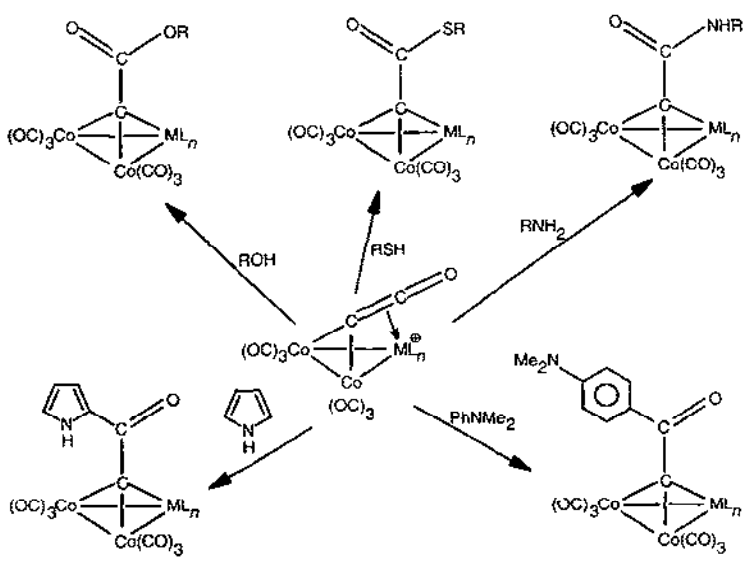

Scheme 7. Reactions of cationic ketenylidene clusters with nucleophiles.

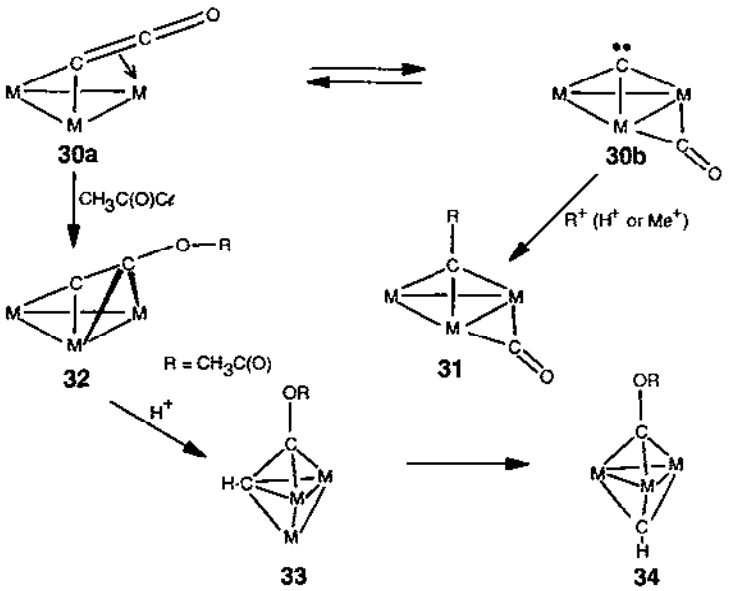

Scheme 8. Reactions of anionic ketenylidene clusters with electrophiles.

which renders the α-carbon sterically inaccessible to the incoming electrophile, but Shriver and coworkers [30] have also shown that EHMO calculations localize the HOMO of **14** on a metal center rather than on the ketenylidene capping group.

The ready migration of the carbonyl fragment of the C=C=O group to the metal triangle as in the purported equilibrium between **30a** and **30b** finds a parallel in the cationic systems. Thus, as mentioned previously, the $AlCl_3$-promoted dechlorination of $Co_3(CO)_9C$–Cl does not yield $[Co_3(CO)_9C]^+$, but rather the carbonyl migration product $[Co_3(CO)_9C$–C=O$]^+$ **5**. (The tenth CO group is provided not by free carbon monoxide, but rather from other sacrificial $Co_3(CO)_9C$–Cl molecules [23].) The reverse process, i.e. migration of a ketonic carbonyl group from a capping position to a terminal metal, has also been reported. Seyferth and Nestle [78] noted that the thermolysis of molecules of the type $Co_3(CO)_9C$–(C=O)Ar resulted in a loss of CO and the formation of the corresponding $Co_3(CO)_9C$–Ar clusters. They raised the possibility of the direct loss of a CO fragment via a radical mechanism or the initial elimination of a metal carbonyl ligand with subsequent migration of the aryl substituent from the β-carbon to the α-carbon of the ketenylidene [78]. These mechanistic proposals were further investigated by Gates et al. [79] who showed, by a series of labelling experiments, that the latter process is in accord with the experimental data, as shown in Scheme 9.

The status of ketenylidene chemistry has been reviewed by Geoffroy and Bassner [80] and it is apparent that there is much that the experimental chemist as well as the theoretician can still contribute to this area.

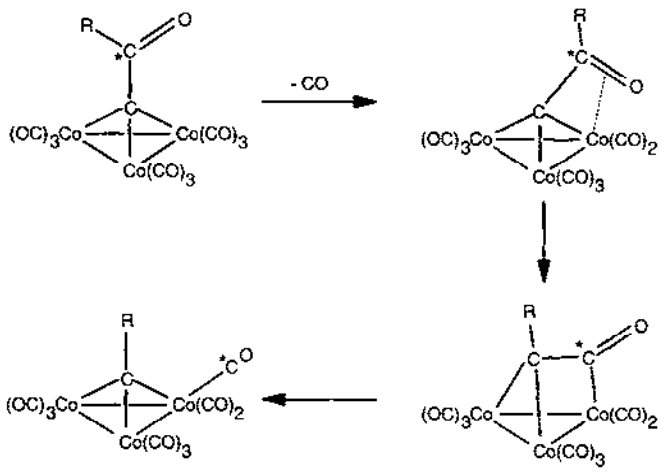

Scheme 9. Mechanism of CO elimination from $Co_3(CO)_9C{-}(C{=}O)Ar$ to give $Co_3(CO)_9C{-}Ar$.

6. Reactivity of $[M_2L_6(RC{\equiv}C{-}CR'R'')]^+$ cluster cations

6.1. Reactions with nucleophiles

The use of $[Co_2(CO)_6(RC{\equiv}C{-}CR_2)]^+$ cluster cations in organic synthesis was first exploited by Nicholas [81], who demonstrated that such reagents can react with a variety of nucleophiles. The synthetic aspects of this elegant chemistry have been comprehensively reviewed by Nicholas [81] and we merely summarize the main themes. Typically, **19** alkylates alcohols or phenols at oxygen, amines at nitrogen and aromatics and other weak nucleophiles at carbon (see Scheme 10).

Indeed, it is not strictly necessary to isolate these cobalt-stabilized cations; in many cases, the electrophile can be generated in situ by the addition of a Lewis acid or a Brønsted acid to the precursor alcohol; subsequent addition of the appropriate nucleophile yields the desired product, as exemplified in Scheme 11 [82,83].

6.2. Relative reactivities of $Co_2(CO)_6$- and $Cp_2Mo_2(CO)_4$-stabilized propargyl cations

Analogous to the behavior of the dicobalt-complexed cations **19**, the molybdenum cluster cation $[Cp_2Mo_2(CO)_4(HC{\equiv}C{-}CH_2)]^+$ (**21**) also reacts with alcohols, amines or thiols [48,52]. However, there is a clear difference in reactivity between the dicobalt cluster cations and their dimolybdenum counterparts. For example, the cobalt cations react with acetone [84] or acetonitrile [85]; in contrast, these can be used as solvents for the molybdenum systems. To gauge the relative reactivities of the Co- and Mo-stabilized cations, they were each allowed to react with 3,4-dimethoxyphenethylamine (**35**), which is a model for dopamine.

As depicted in Scheme 12, both cations react with **35** to give a mixture of mono- and di-*N*-alkylated products; however, when the amino functionality was protected

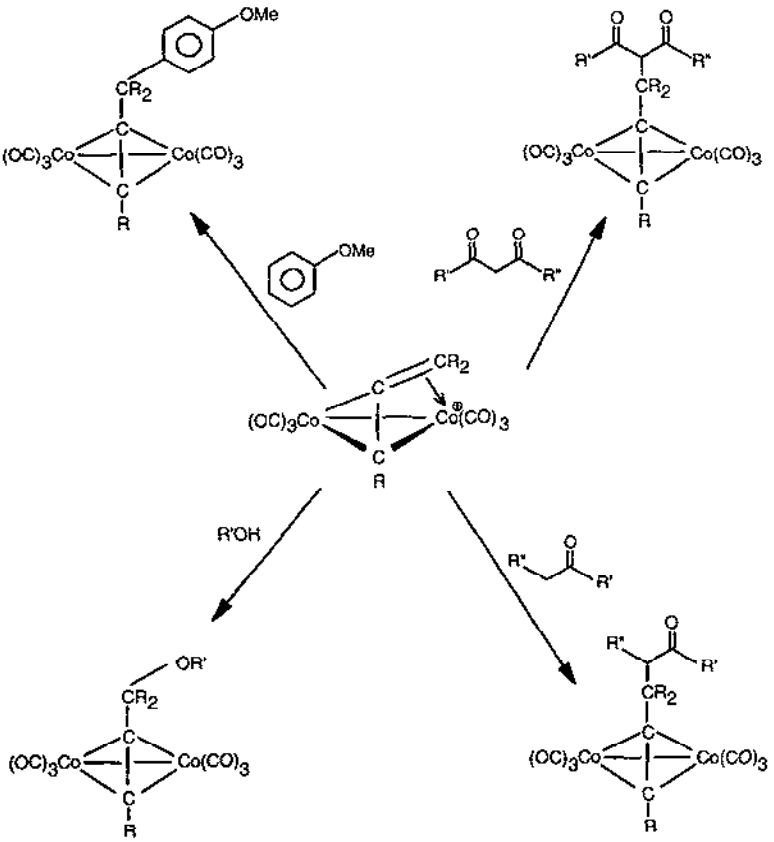

Scheme 10. Reactions of $[(propargylium)Co_2(CO)_6]^+$ clusters with nucleophiles.

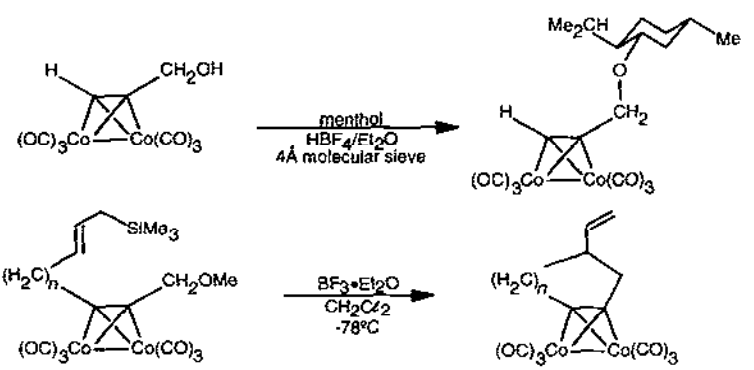

Scheme 11. Typical examples of the use of propargylium cations **19** as intermediates in organic synthesis.

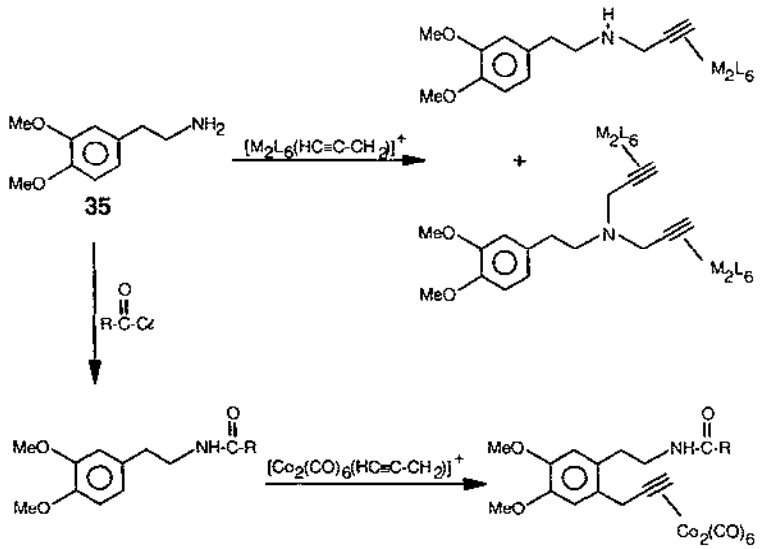

Scheme 12. Reactions of the cobalt or molybdenum cations, **19** and **21** respectively, with 3,4-dimethoxyphenethylamine (**35**).

as an amide, attack on the aromatic ring was observed [86]. The difference is that, while the cobalt cation is restricted to organic solvents such as dichloromethane, the dimolybdenum cation **21** can be used in protic biphasic media. Moreover, the reaction of $[Cp_2Mo_2(CO)_4(HC{\equiv}C{-}CH_2)]^+$ with the amine **35** in methanol is markedly pH dependent. At low pH (pH 1.9), the amine is entirely protonated and *O*-alkylation is the sole reaction; in contrast, at pH 3.3, *N*-alkylation is competitive and proceeds to the extent of 50%. The significance of this result is that it is now possible to attach organometallic labels to biomolecules in aqueous media. (We shall return to these important applications of cluster cations in Section 9.)

Overall, the greater reactivity of the cobalt cations is counterbalanced by the more selective nature of the molybdenum cationic complexes. This behavior can be rationalized in terms of the reported pK_R^+ values of these ions which characterize the following equilibria [41,60]

$$[M_2L_6(HC{\equiv}C{-}CH_2)]^+ + 2H_2O \rightleftharpoons M_2L_6(HC{\equiv}C{-}CH_2OH) + [H_3O]^+$$

When $M_2L_6 \equiv Co_2(CO)_6$, $pK_R^+ \approx -6.8$ to -7.2; for $M_2L_6 \equiv Cp_2Mo_2(CO)_4$, $p > K_R^+ \approx +3.4$ this tells us that the cobalt-stabilized cations can exist in aqueous medium only at very low pH (pH < 1), whereas the Mo-stabilized systems can survive at much higher pH values. This very large difference of approximately 10^{10} in the K_R^+ values testifies to the much greater relative stability of the molybdenum derivatives [86]. As we shall see presently (Section 7), it is possible to compare directly the cation-stabilizing abilities of $Co(CO)_3$ and $CpMo(CO)_2$ vertices by incorporating both groups into the same cluster.

6.3. Heteroatom-stabilized cluster cations

The high reactivity of $Co_2(CO)_6$-stabilized propargyl cations can be problematic in terms of selectivity and storage for later use. Jaouen and coworkers [87] chose to address this issue by treating $[Co_2(CO)_6(HC{\equiv}C{-}CH_2)]^+$ (**19**) with a number of sulfides and phosphines, and with pyridine. The complexes $[Co_2(CO)_6(HC{\equiv}C{-}CH_2SR_2)]^+$ (**36**), where R ≡ Me, Et or ^{i}Pr, are readily isolable and react with nucleophiles such as water, methanol or anisole. However, their reactivity is somewhat attenuated compared with that of **19**. The cations $[Co_2(CO)_6(HC{\equiv}C{-}CH_2py)]^+$ (**37**) and $[Co_2(CO)_6(HC{\equiv}C{-}CH_2PEt_3)]^+$ (**38**) are also stable; indeed, the latter has been characterized by X-ray crystallography. Very recently, the corresponding molybdenum complex $[Cp_2Mo_2(CO)_4(MeC{\equiv}C{-}CH_2PEt_3)]^+$ has also been synthesized and its X-ray crystal structure reported [88]. It is evident that, in these systems, there is no longer a direct interaction between the β-carbon and a metal vertex; moreover, a substantial fraction of the positive charge is located on the heteroatom. Preliminary kinetic data suggest that the reaction of $[Co_2(CO)_6(HC{\equiv}C{-}CH_2SEt_2)]^+$ with MeOH proceeds via an S_N2 mechanism, whereby the SEt_2 moiety functions as the leaving group [87]. It is noteworthy that, without the protecting $Co_2(CO)_6$ unit, propargylic sulfonium and phosphonium salts isomerize in solution to give the corresponding allenes [89,90].

6.4. Metal-stabilized dications

These sulfide-stabilized cationic cobalt clusters have been exploited by Went and coworkers [91,92] to construct cycloalkynes containing sulfur and oxygen.

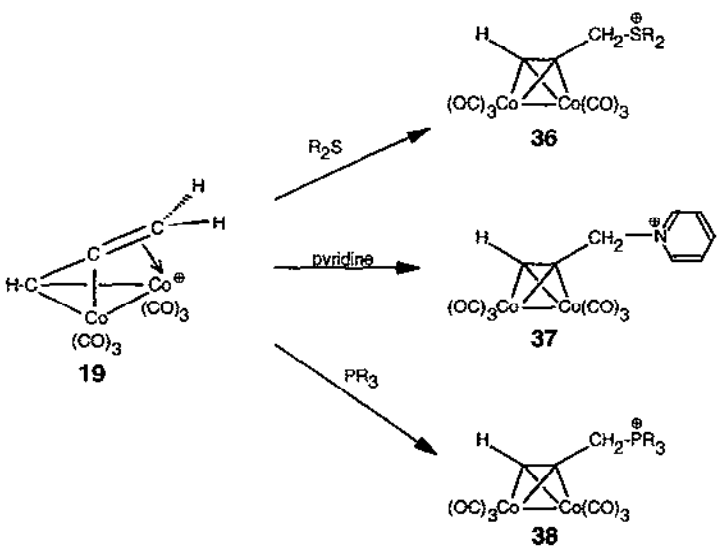

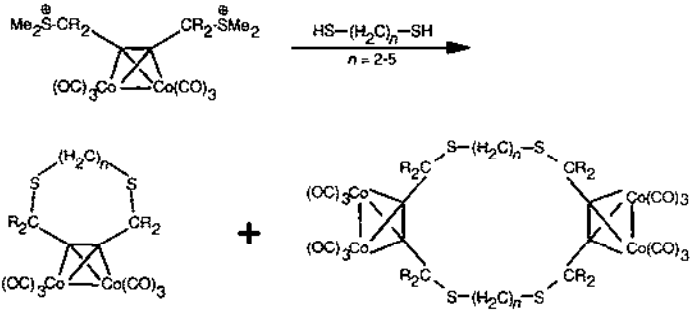

Scheme 13. Use of sulfide-stabilized dications to generate heterocycles.

Protonation of $Co_2(CO)_6(HOCH_2C{\equiv}C{-}CH_2OH)$ with HBF_4–ether in the presence of dimethyl sulfide gives $[Co_2(CO)_6(Me_2S{-}CH_2C{\equiv}C{-}CH_2{-}SMe_2)]^{2+}$ as air and thermally stable orange crystals. This dication reacts with $HS(CH_2)_nOH$ or $HS(CH_2)_nSH$, where $n=2$–5, to give the corresponding heterocycles, as in Scheme 13.

Very recently, Went and coworkers [93] have extended this synthetic methodology to the preparation of alkylamine complexes. The normal acid-catalyzed route to $[Co_2(CO)_6(CH_2C{\equiv}C{-}CH_2)]^{2+}$ is unsuitable for reaction with basic amines, since RNH_3^+ would be generated. However, isolation of $[Co_2(CO)_6(Me_2S{-}CH_2C{\equiv}C{-}CH_2{-}SMe_2)]^{2+}$ and subsequent treatment with diphenylamine provides an efficient route to $Co_2(CO)_6(Ph_2N{-}CH_2C{\equiv}C{-}CH_2{-}NPh_2)$ [93]. An alternative approach to stabilizing the propargyl cations is to enhance the electron density at the metal centers by replacing CO ligands by phosphines. Thus Went and coworkers have found that substitution of four carbonyls by two diphenylphosphinomethane (dppm) ligands yields the stable dication $[Co_2(CO)_2(dppm)_2(CH_2C{\equiv}CCH_2)]^{2+}$ (**39**) when treated with HBF_4. Again, this dication is a convenient reagent with which to prepare difunctionalized alkynes [93].

In a very recent development, Curtis and coworkers [94] have successfully characterized the dicationic salt $[Cp_2Mo_2(CO)_4(CH_2C{\equiv}CCH_2)]^{2+}\ 2[BF_4]^-$ (**23**) by X-ray crystallography. The dication **23** adopts a C_2 structure and the Mo–C^+ distances average 2.46 Å, typical for a primary cation [52,53].

This dication has also been the subject of a molecular orbital investigation which showed the LUMO to be primarily a metal-based orbital [94]. In contrast, in the monocation $[Cp_2Mo_2(CO)_4(HC{\equiv}CCR_2)]^+$, the LUMO is largely localized at the cationic center and reduction with sodium yields a radical which couples to give the dimer **40** [58,95].

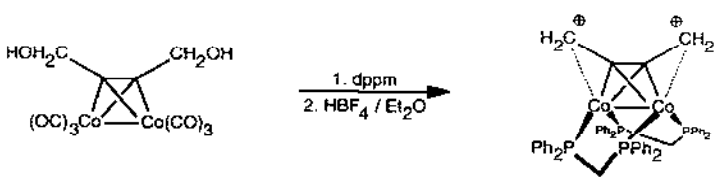

39

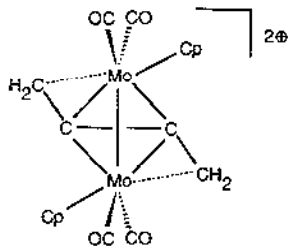

23

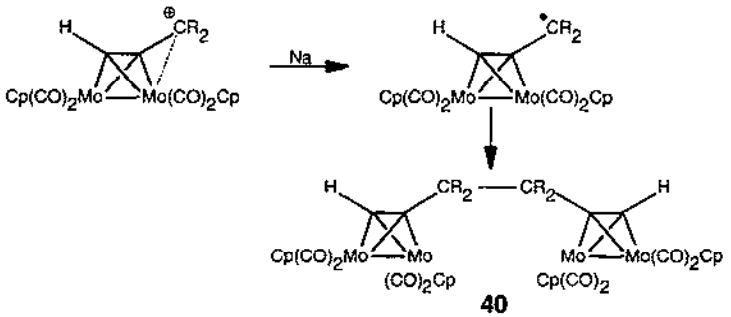

40

7. Mixed-metal cluster cations

7.1. The stereochemistry of cation formation

The ready isolation of dimolybdenum cations, together with the reported pK_R^+ values previously discussed, suggest that, in a direct competition between $CpMo(CO)_2$ and $Co(CO)_3$ vertices, a cationic center would be preferentially stabilized by the former. This was first investigated by D'Agostino et al. [36] who prepared the mixed-metal clusters $CpMCo(CO)_5(HC{\equiv}CCH_2OH)$ (**41**) (M ≡ Mo or W), which on protonation furnished the cations $[CpMCo(CO)_5(HC{\equiv}CCH_2)]^+$ (**42**). The ^{13}C NMR chemical shifts of the metal carbonyls indicated strongly that the positive charge was partially delocalized onto the molybdenum (or tungsten) atom, while the cobalt carbonyls were little affected. (It is straightforward to assign ^{13}CO ligands bonded to tungsten by means of the satellite peaks caused by the 14% abundant ^{183}W isotope.)

These spectroscopic data were supplemented by EHMO calculations (see Fig. 13) which likewise indicated a more favorable interaction with the Mo vertex (**42a**) rather than with the $Co(CO)_3$ group (**42b**). Variable-temperature NMR studies indicated that these were not fluxional molecules; unlike the homodimetallic systems $[Co_2(CO)_6(HC{\equiv}CCH_2)]^+$ or $[Cp_2Mo_2(CO)_4(HC{\equiv}CCH_2)]^+$, for which the antarafacial migration pathway has been firmly established [42,43,50–55], there was no evidence for the formation of a cobalt-stabilized isomer (**42b**).

Interestingly, when the secondary alcohol $CpWCo(CO)_5(HC{\equiv}CCH(Et)OH)$ (**43**)

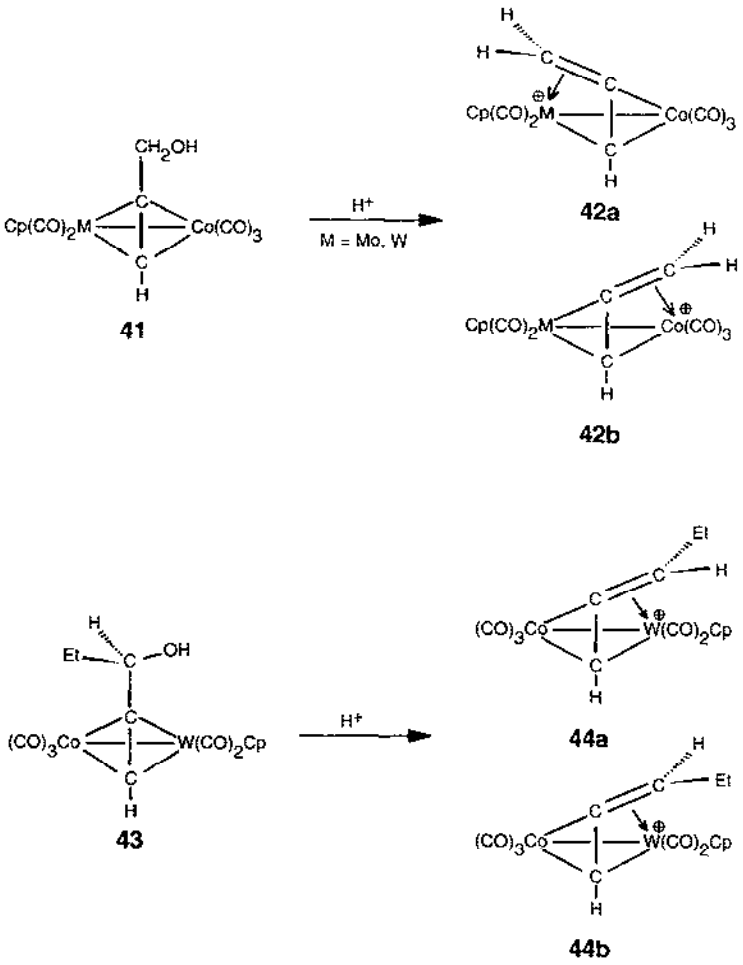

was protonated, two diastereomers **44a** and **44b** were observed in a 2:1 ratio [36]. Moreover, an important series of experiments by Nicholas and coworkers [96] revealed an even more striking example of diastereoselectivity. It was shown that the substitution of a carbonyl ligand in a $Co(CO)_3$ vertex by a phosphine group not only enhanced the stabilizing ability of the cluster, but also yielded a cation in which the vinylidene capping fragment interacted preferentially with the $Co(CO)_2PR_3$ vertex. When the diastereomers of $Co_2(CO)_5PPh_3(HC{\equiv}C{-}CH(^tBu)OH$ (**45a** and **45b**) were protonated, only a single cation **46a** was produced. It is apparent that the structure of this product minimizes the steric interactions between the ^{t}Bu groups and the other cluster vertices, but the routes to this product from two isomeric precursors must be different [97].

The explanation which has been advanced [98] is depicted in Scheme 14. It is assumed that these cations are generated by initial protonation of the alcohol

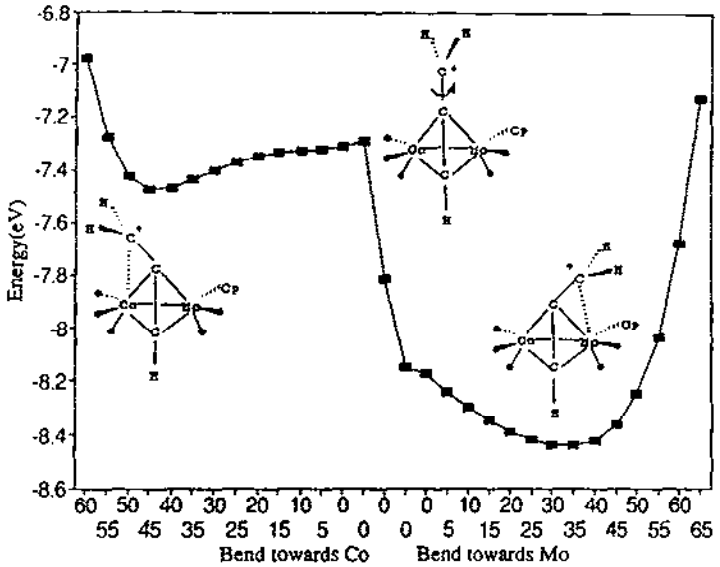

Fig. 13. EHMO-calculated energy profile depicting the preferential interaction of a methylene fragment with a $CpMo(CO)_2$ vertex (as in **42a**) rather than with a $Co(CO)_3$ unit (**42b**).

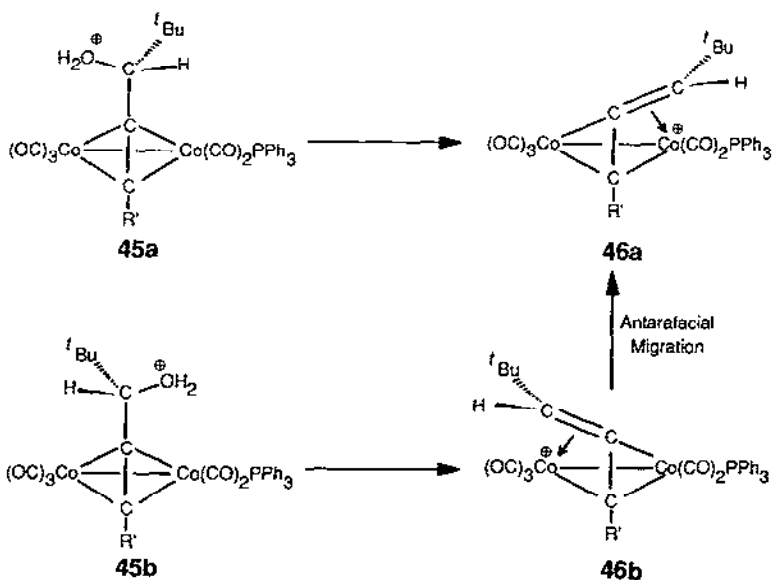

Scheme 14. Proposed mechanism to account for the observation of a single diastereomer **46a** generated via antiperiplanar elimination of water from two isomeric precursors **45a** and **45b**.

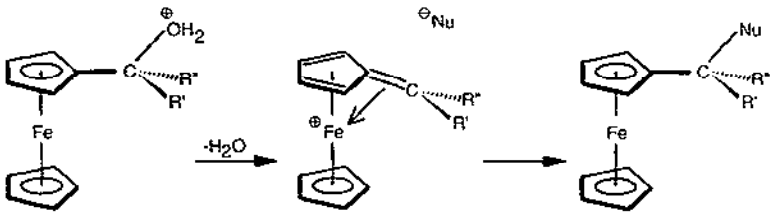

Scheme 15. Nucleophilic substitution in a chiral ferrocenylmethanol occurs with retention of configuration.

precursor and that loss of water occurs with anchimeric assistance from a metal center which is antiperiplanar with respect to the leaving group. Certainly, this mechanism is well established for $Cr(CO)_3$-stabilized benzyl cations [99] or ferrocenylmethyl cations [100] which undergo substitution with retention of configuration, as exemplified in Scheme 15.

Now, if we assume that elimination of water can be assisted either by the $Co(CO)_2PR_3$ or the $Co(CO)_3$ vertex, then clearly two isomeric cations can result. However, if cation **46b** (which is stabilized by the $Co(CO)_3$ moiety) can undergo irreversible antarafacial migration to the more stable isomer **46a**, then only a single product will result. This same reasoning may be applied to the Co–W cations **44a** and **44b**, whereby the minor percentage of cation generated in a cobalt-assisted transition state can irreversibly isomerize to the favored W-stabilized diastereomer [36,98].

7.2. *Mixed-metal cluster cations derived from terpenes*

Terpenoid cations hold a pivotal position in the history of molecular rearrangements [101]. The Wagner–Meerwein skeletal rearrangement of camphenyl chloride to isobornyl chloride is a classic example of a 1,2-alkyl shift [102], and is depicted in Scheme 16.

In contrast, the electronically disfavored 2-alkynylbornyl cation **47** undergoes a Wagner–Meerwein rearrangement in the opposite sense so as to generate a camphenyl cation **48**; a subsequent methyl shift yields **49** which itself suffers Wagner–Meerwein rearrangement to regenerate the sterically favored bornyl skeleton **50** [103], as in Scheme 17.

D'Agostino et al. [36,83] realized that this system offered an opportunity to stabilize the 2-alkynylbornyl cation as its $Co_2(CO)_6$ or $Cp_2Mo_2(CO)_4$ complex (**51** and **52** respectively). These complexes were prepared and characterized by two-dimensional NMR techniques which revealed that no skeletal rearrangement of these

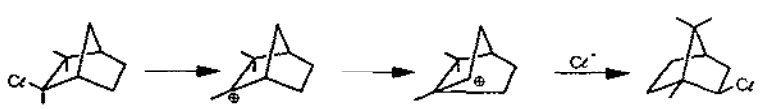

Scheme 16. Wagner–Meerwein rearrangement of camphenyl chloride to isobornyl chloride.

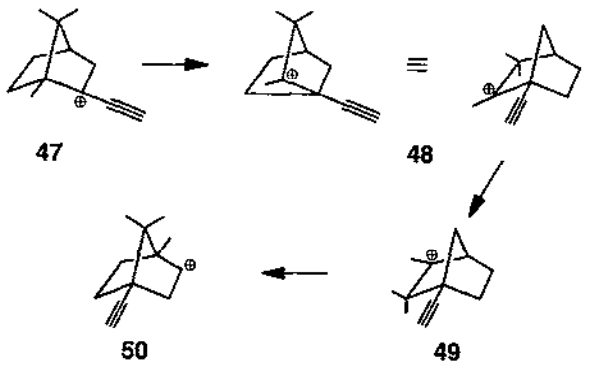

Scheme 17. Wagner–Meerwein rearrangement of the 2-ethynylbornyl cation to the 4-ethynylbornyl cation.

cations had occurred. They were also able to prepare the mixed molybdenum–cobalt cluster cation **53**, whose NMR spectrum indicated it to be stabilized by preferential interaction with the $CpMo(CO)_2$ vertex.

The cations **52** and **53** were later characterized by X-ray crystallography, and this provided the first unequivocal structural evidence that the cations were indeed preferentially bonded to the molybdenum center [61]. Since it was now firmly established that metal clusters could stabilize a terpenoid cation against Wagner–Meerwein rearrangement, the next aim was to elucidate the limits of this interaction. The question arose as to whether the cluster could prevent the rearrangement of a terpenoid cation which was under considerable steric pressure to isomerize. For this purpose, Gruselle and coworkers [62] prepared and protonated the $Co_2(CO)_6$ complex of 2-propynylfenchol (**54**) shown in Scheme 18. In this system, an equilibrium is set up between the initial cation **55** and its Wagner–Meerwein isomer **56**. On quenching the mixture with water, cation **55** forms the alcohol **57**, the epimer of **54**; meanwhile, the rearranged cation **56** yields primarily a mixture of elimination products, **58** and **59**. Replacement of a $Co(CO)_3$ moiety in the alkene **58** with $CpMo(CO)_2$ gives one almost pure diastereomer **60** which, on protonation to give **61**, undergoes Wagner–Meerwein rearrangement back to the original fenchyl skeleton **62** which has been characterized X-ray crystallographically.

The message from this chemistry is clear. A sterically encumbered fenchyl cation, even when stabilized by coordination to a $Co(CO)_3$ cation, is unable to resist the

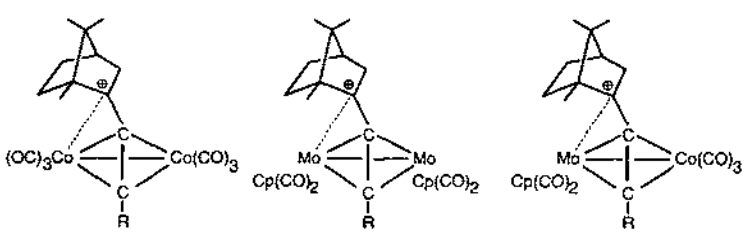

51 **52** **53**

cationic rearrangement to the less crowded bornyl skeleton. However, when the bornyl cation **61** has the opportunity to be stabilized by a molybdenum center, it undergoes Wagner–Meerwein rearrangement to **62** even though it must adopt the sterically disfavored fenchyl structure.

These data allow us to begin constructing a hierarchy of organometallic fragments in terms of their ability to stabilize carbocationic centers. A number of organometallic cations have been isolated and characterized spectroscopically and/or structurally. Typically, it has been shown by NMR and X-ray crystallography that, in the cluster $[(C_5H_5)Fe(C_5H_4)\text{–}CH\text{–}(C{\equiv}CR)Mo_2(CO)_4Cp_2]^+$ (**63**), it is the molybdenum cluster rather than the ferrocenyl fragment which preferentially stabilizes the electron-

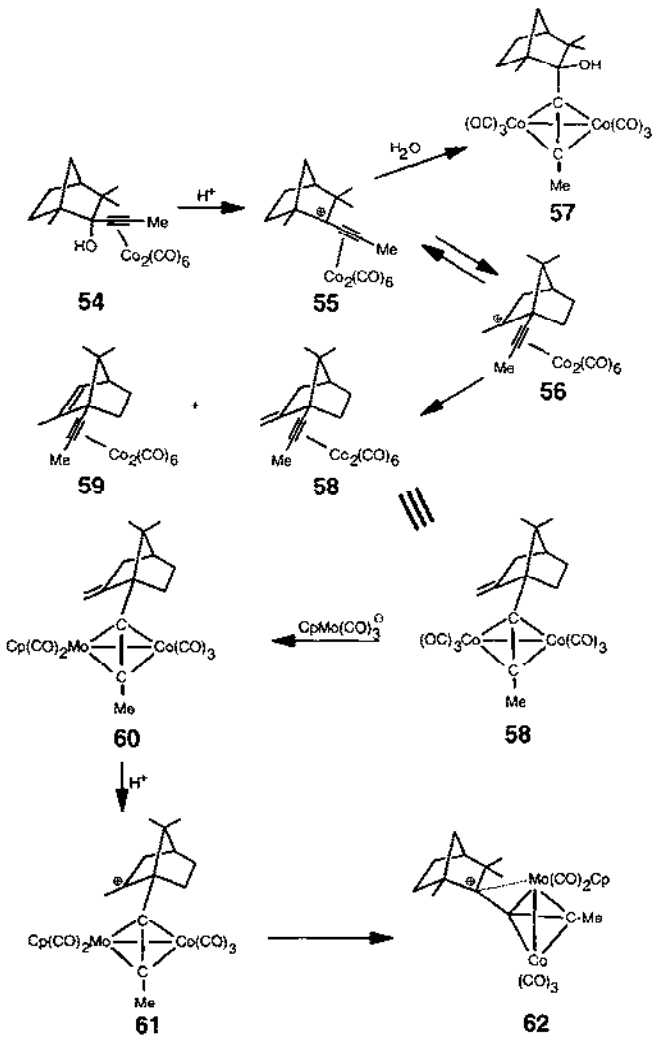

Scheme 18. Wagner–Meerwein rearrangements in the fenchyl system.

deficient center [59]. It is perhaps more realistic to visualize these metal-stabilized carbocations as vinylidene groups coordinated to an M_3 or M_2C triangle [19,24,32,44]. We are aware of several other systems (**64–67**) [44,104–106] in which a C=CR′R″ moiety can selectively bind to its preferred metal fragment. Thus, in a preliminary fashion, we can begin to arrange metal vertices in order of their ability to stabilize carbocationic centers. Molecules **63** and **64** tell us that $Cp_2Mo_2(CO)_4(RC{\equiv}C{-})$ > ferrocenyl > $Co_2(CO)_6(RC{\equiv}C{-})$. Furthermore, we can see from molecules **65–67**, and also from **16**, **17**, **44** and **46**, that CpRu > CpFe and $Ru(CO)_3$ > $Fe(CO)_3$ > $CpW(CO)_2$ > $Co(CO)_2PPh_3$ > C o$(CO)_3$.

8. Cyclizations mediated by dicobalt cluster cations

The ability of cobalt-stabilized propargyl cations to promote cyclization reactions has been briefly discussed in Section 6.1. Recently, cobalt-promoted Friedel–Crafts alkylations on electron-rich aromatic rings have been exploited for synthetic purposes [107]. On treatment of the alkynols **68a** or **68b** with BF_3-etherate, the tricyclic

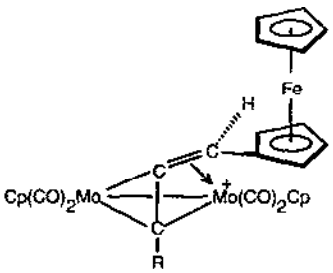

63

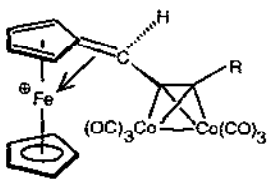

64

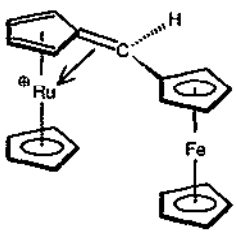

65

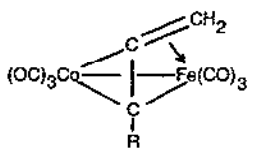

66

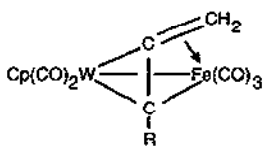

67

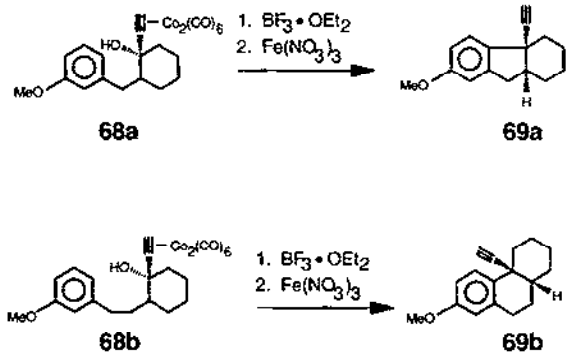

products **69a** and **69b** respectively are obtained. Electrophilic attack on the aromatic ring produces a new five- or six-membered ring; more impressively, the predominant cyclization product in each case is the one in which the newly formed ring has a cis ring junction with the existing six-membered ring.

This stereochemical control results from the mode of attack by the relatively electron-rich arene at the cationic center in **70**. As indicated in Fig. 14, the nucleophile must approach the cation from the face opposite to the site of attachment of the cobalt. Since the bulky Co_2C_2 cluster preferentially occupies an equatorial site in the final product [108], the trajectory of approach by the incoming aromatic ring must be pseudo-axial, as in **71**. This in turn requires that the benzyl substituent in the cationic intermediate **70a** (or the phenethyl substituent in **70b**) be sited equatorially. The relative orientations of the benzyl (or phenethyl) and hydroxyl functionalities in the starting material **68** are irrelevant, since the intermediate cobalt-stabilized cation **70** can simply undergo an antarafacial migration from one cobalt to the other to generate the required conformation for cyclization.

Fig. 15 illustrates the favored transition state for cyclization to a six-membered ring. The nucleophile approaches axially in such a manner that the hydrogen bonded to the attacking aryl carbon is oriented trans to the tetrahedral cluster, thus allowing

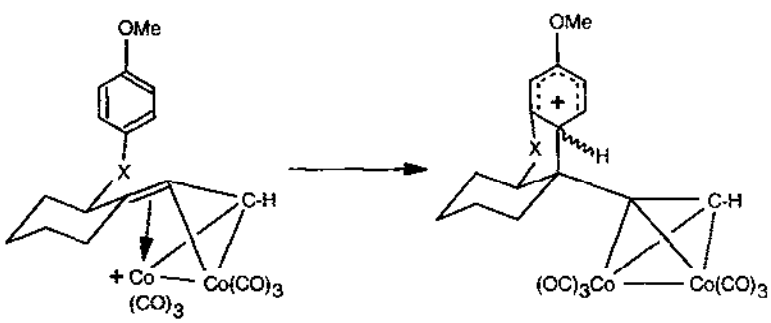

Fig. 14. Nucleophilic attack by an arene on a cobalt-stabilized cation.

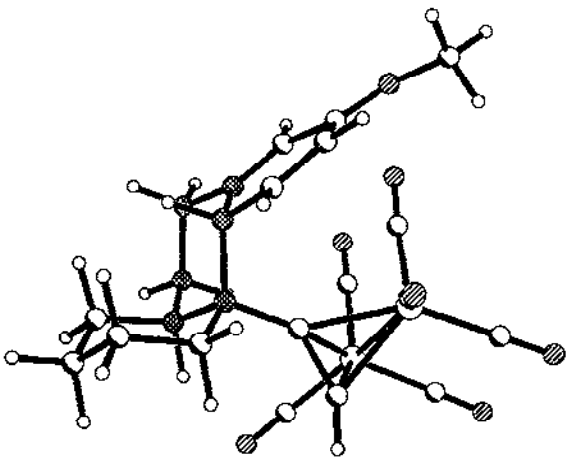

Fig. 15. PC-MODEL-derived transition state, **71b**, showing the favored chair-like conformation of the newly formed six-membered ring; for clarity, the six atoms which make up the chair are cross-hatched.

the newly formed six-membered ring to adopt the favored chair conformation in the transition state.

It is relevant to note that Nicholas and coworkers [109] have offered a similar rationale for their elegant $Mn(OAc)_3$-mediated oxidative cycloaddition reactions of β-dicarbonyl compounds with $Co_2(CO)_6$-complexed 1-alkene-3-ynes. In these cases, it is believed that the initially generated radicals are oxidized to cations prior to ring closure.

9. Bio-organometallic applications of steroidal organometallic cations

The use of organometallic markers in biological systems is a topic of burgeoning importance. Of particular relevance to this review are the contributions of Jaouen et al. [110] concerning the carbonylmetalloimmunoassay (CMIA) technique. The CMIA approach seeks to avoid the use of radioactive labels to assay hormonal receptor sites; these assays play a crucial role in the detection and treatment of certain types of breast cancer for which the mechanism of development is hormone dependent [111]. The pivotal factor in such studies is the recognition of a particular protein receptor by a biological molecule even when it is modified by the incorporation of the organometallic fragment [112]. Conventional approaches use radiolabelled estrogens to bind to the receptor site and the assay is accomplished by radiochemical techniques. Jaouen's achievement was to demonstrate that estradiol derivatives bearing metal carbonyl fragments provide a convenient method of assaying the estradiol receptor sites. In this case, the probe is the intensity of the metal carbonyl ν_{CO} vibrations which absorb strongly in the region 2100–1850 cm^{-1}—a window in which proteins do not absorb.

In the early stages of this work, the metal carbonyl fragment was attached to the

aromatic A ring of the steroid [113], but the relative binding affinities (RBAs) were too low for these molecules to be used in bioassays [114]. (The RBA value is a quantitative measure of the ability of the molecule in question to attach itself to the specific receptor site; the natural hormone, estradiol, is assigned a value of 100%.) The most effective systems found were those which possessed a 17α-alkynyl functionality, as in mestranol (**72**) or RU 486 (**73**), the controversial "morning-after pill" which is currently licensed for use in France and China. The $Co_2(CO)_6$ and $Cp_2Mo_2(CO)_4$ complexes of these steroidal alkynes (**74**) have been synthesized and shown to possess acceptably high RBA values. Moreover, the rhenium derivative **75** has an RBA value of 172%, and is the first steroidal organometallic to bind more efficiently than estradiol itself [115].

The particular feature of relevance here is that several of these complexes, notably **74**, where ML_n is $Co(CO)_3$, induce irreversible covalent binding to the estrogen receptors [116], i.e. they can function as affinity markers. The key step is the transformation of the 17β-OH functionality into the corresponding carbenium ion which is stabilized by the neighboring transition metal cluster fragment. The nucleophilic sulfur residues of a coordination unit involving an acidic metal (presumably Zn^{2+}), cysteines 530 and 381 and histidines 524 and 516 (human estrogen numbering) in close proximity to the estradiol binding site are good candidates for the establishment of such a covalent bond and the consequent receptor inactivation [110]. In support of the hypothesis that 17β-OH plays a crucial role in these interactions, the isoelectronic complex $[FeCo(CO)_6]$(17α-ethynyl-17β-dehydroxyestradiol) (**76**) was shown to be completely ineffective as an affinity marker [44].

A number of steroidal organometallic cations have now been characterized and their chemistry has been investigated. Nicholas and Siegel [117] prepared the $Co_2(CO)_6$ complexes of both mestranol and epi-mestranol, but protonation and subsequent borohydride reduction yielded the same product in both cases. Evidently,

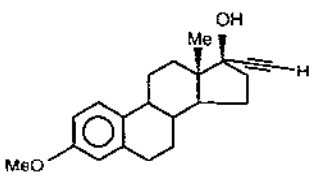

72

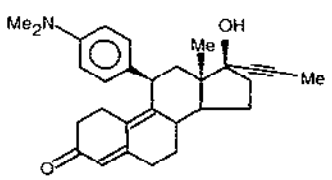

73

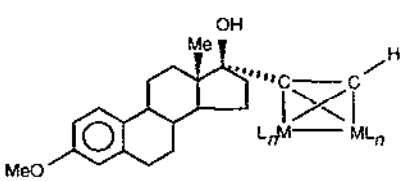

$L_nM = (OC)_3Co$; $Cp(CO)_2Mo$

74

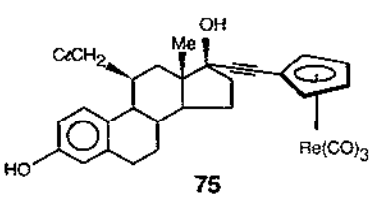

75

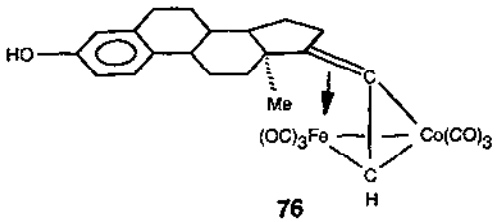

76

these reactions proceed through a common cation, **77**, and borohydride attack must occur on the α-face of the steroid, as shown in Scheme 19.

The analogous dimolybdenum cluster cation **78** has been characterized by X-ray crystallography; one Mo interacts directly with the β-face of the steroid, thus leaving

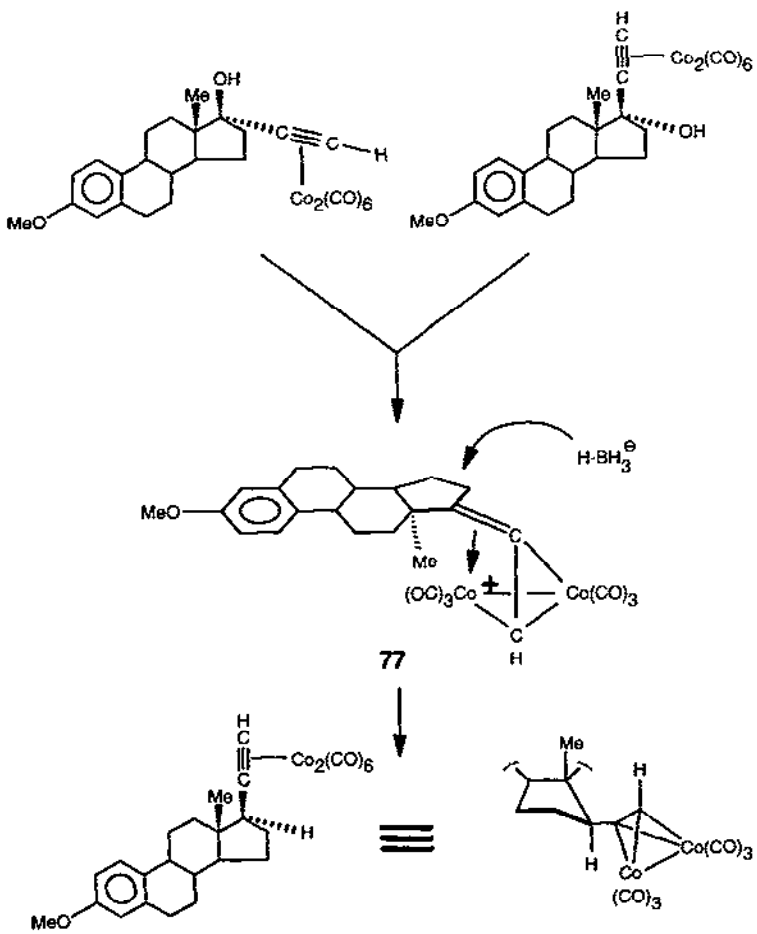

Scheme 19. Borohydride reduction of the steroidal dicobalt cation 77 leading to a single product in which the cluster occupies a pseudo-equatorial site in the five-membered ring.

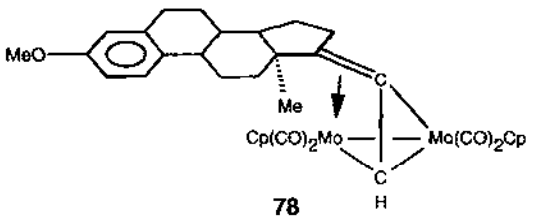

78

the α-face open for an incoming nucleophile [60]. Interestingly, the dicobalt cation **77** suffers methyl migration and subsequent elimination to yield a mixture of alkenes [60]. Indeed, these ready eliminations to form alkenes are frequently problematic with cobalt cations, since they seriously reduce the yields of the nucleophilic addition product. The most convenient way to avoid these unwanted eliminations or other side reactions is to generate the cation in the presence of Me_2S, as described previously in Section 6.3.

10. The isolobal relationship between $Co(CO)_3^+$ and $Fe(CO)_3$

We have noted already in Section 3.1 that formally it is possible to replace a $Co(CO)_3^+$ vertex in a cluster by an isolobal $Fe(CO)_3$ unit. Indeed, it has been reported [44] that the X-ray crystallographically determined geometry of $(MeC{\equiv}C{-}CH_2)FeCo(CO)_5PPh_3$ is in close accord with the calculated minimum energy structure for $[(HC{\equiv}C{-}CH_2)Co_2(CO)_6]^+$, for which no X-ray data are currently available. This concept can be extended to predict the structure of the dication $[(CH_2{-}C{\equiv}C{-}CH_2)Co_2(CO)_6]^{2+}$ (**79**) for which the neutral molecule $(CH_2{=}C{=}C{=}CH_2)Fe_2(CO)_6$ (**80**) provides a model. The structure of **80** is known from X-ray data [118]; the molecule adopts a C_2-type geometry, closely analogous to the recently described structure of the molybdenum dication **23** [94].

The neutral $Fe(CO)_3$ analogues of the $Co(CO)_3^+$ cationic clusters can be prepared directly from cobalt precursors. Thus the treatment of (propargyl alcohol)$Co_2(CO)_6$ with $Fe(CO)_5$ in refluxing acetone yields $(HC{=}C{-}CH_2)FeCo(CO)_6$ (**81**); this same reaction is also applicable to the diol $(HOCH_2{-}C{\equiv}C{-}CH_2OH)Co_2(CO)_6$ which, on treatment with $Fe(CO)_5$, gives $(CH_2{=}C{=}C{=}CH_2)Fe_2(CO)_6$ (**80**) [119]. The mechanism of this conversion has not been established, but it is known that $Co_2(CO)_8$ and $Fe(CO)_5$ in acetone lead to the formation of $HFeCo_3(CO)_{12}$ [120]. Thus the

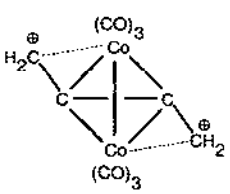

79

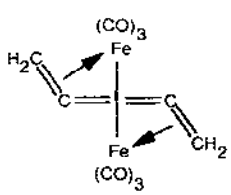

80

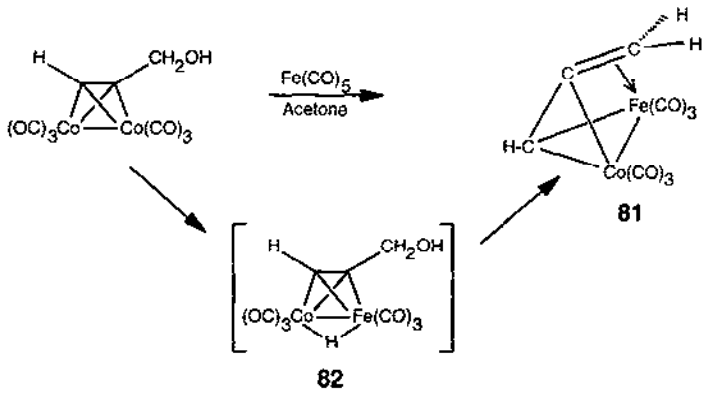

transformation of (propargyl alcohol)$Co_2(CO)_6$ into $(HC{\equiv}C{-}CH_2)FeCo(CO)_6$ may involve the formation of an intermediate metal hydride **82** and the subsequent elimination of water.

It is tempting to push this analogy further, even into the five-atom square-based pyramidal clusters reported by Wojcicki and coworkers [106] and Mathieu and coworkers [121]. Typically, they have crystallographically characterized the clusters **83** and **84**, which they describe as allenyl complexes. An alternative view would be to classify them as nido clusters, in which a methylene moiety interacts directly with an $Fe(CO)_3$ vertex. The isolation of these molecules suggests that the corresponding cobalt cationic systems **85** and **86** should be able to be prepared from the precursor alcohols. Indeed, we may also wonder whether these latter cobalt systems may function as precursors to the iron complexes. Clearly, there remains much to do in this area!

11. Future prospects

11.1. Cyclopropyl cations

The majority of the cluster-stabilized cations which we have discussed involve dimetallic or trimetallic tetrahedral systems in which the carbocationic center is stabilized by interaction with one or more organometallic vertices. Since carbocations are frequently invoked as short-lived species in organic transformations, we can envisage many cases where a purported intermediate might be trapped as a cluster cation and examined at leisure. For example, cyclopropyl cations normally undergo ring opening to yield the corresponding allyl cation, but a recent NMR study on the ferrocenyl–cyclopropyl system (**87**) presents very strong evidence for the existence of a metal-stabilized cyclopropyl cation [122]. Since we have presented ample evidence that $[(RC{\equiv}C{-}CR_2)Mo_2(CO)_4Cp_2]^+$ cations are not only more stable than their ferrocenyl analogues, but also frequently yield X-ray quality crystals, it would

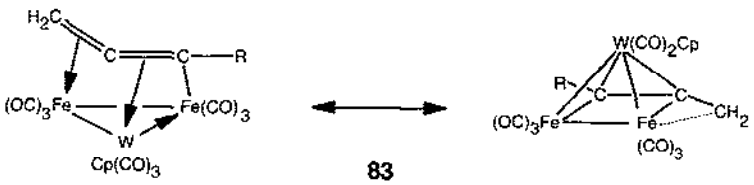

83

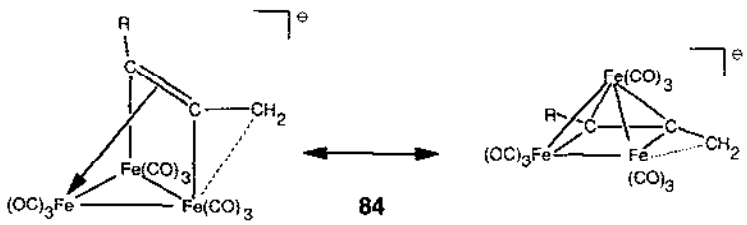

84

85 86

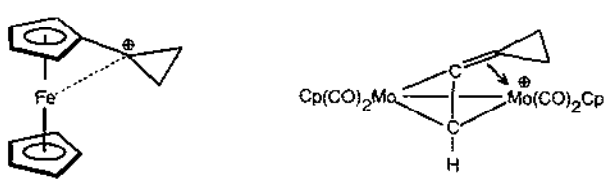

87 88

seem reasonable that a synthesis of $[(HC{\equiv}C\text{-cyclopropyl})Mo_2(CO)_4Cp_2]^+$ (**88**) might yield unequivocal structural data on this system.

11.2. Cluster-promoted cationic rearrangements

The ease of generating cluster-stabilized cations has been exploited by Top and Jaouen [85], who used this technique to bring about reactions under very mild conditions (see Scheme 20). Typically, they showed that the readily accessible cobalt-stabilized propargyl cation **19** reacts with acetonitrile to form the *N*-alkyl nitrilium ion **89** which, on hydrolysis, yields the corresponding amide. It is evident that the presence of the cluster fragment greatly facilitates the formation of the initial cation

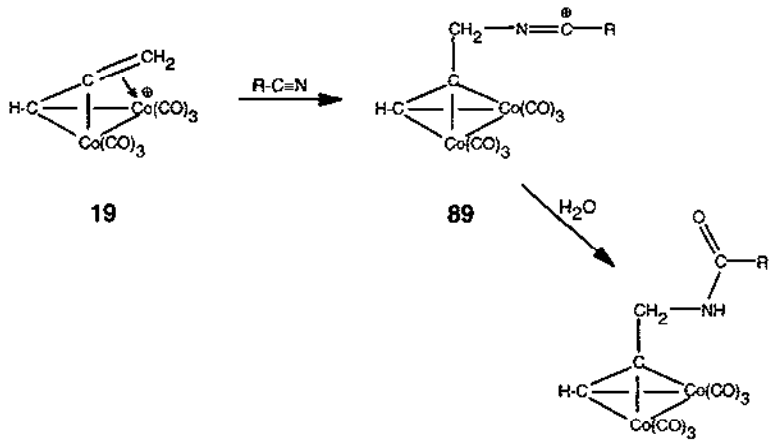

Scheme 20. A cluster-promoted Ritter reaction.

required for the Ritter reaction. Moreover, such an approach has general applicability, since nitrilium ion intermediates are formed in the Beckmann rearrangement process. We can envisage increased usage of such metal-stabilized intermediates in organic synthesis.

11.3. Silylium cations

The recent well-publicized efforts [123,124] to obtain X-ray data on free silylium cations (R_3Si^+, where R ≡ ethyl or isopropyl) raise the obvious possibility that such species could be stabilized by complexation to a transition metal cluster. There are already numerous examples of sp^2-hybridized silicon centers bonded to transition metals [125]. In effect, it would be necessary to construct a silicon analogue of the cluster-stabilized cations that we have discussed at length. Preliminary attempts to achieve this goal have been undertaken, and the potential silylium ion precursor **90** has been synthesized and characterized crystallographically [126]. The problem still remains of generating the SiR_2^+ center in the presence of a non-nucleophilic counter-ion, but a number of such anions are now available [127].

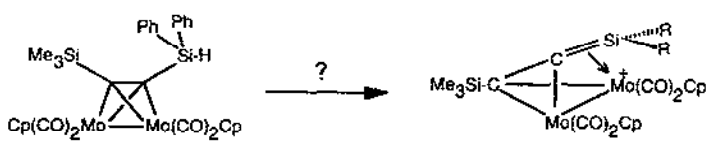

90

11.4. $[(Benzyl)M_3L_n]^+$ cations

A particularly exciting new development involves the stabilization of a benzyl cation on a metal triangular base. While a wide variety of arenes are known to coordinate in an $\eta^2{:}\eta^2{:}\eta^2$ fashion to the Co_3Cp_3 or $Os_3(CO)_9$ fragments [128], it is only recently that evidence has been presented for the generation of the cation $[(\mu^3\text{-benzyl})Co_3Cp_3]^+$ (**91**) [129]. It is to be hoped that crystallographic data on this or a related molecule may become available so as to clarify the interaction of the cationic center with the metal triangular base.

12. Inorganometallic clusters derived from cationic precursors

We cannot conclude without mentioning some of the most esthetically pleasing molecules to have emerged in recent years; they possess an inorganic core and a peripheral coating of cluster moieties. The first such inorganometallic cluster (**92**) was reported by Schore and coworkers [130] as the result of a serendipitous reaction of $[Co_3(CO)_9C{-}C{=}O]^+$ (**5**) with ice–water. Since that time, Fehlner and coworkers [131–134] have devised rational syntheses of a variety of beautiful molecules (**93–96**) in which the conventional acetate bridges have been replaced by $Co_3(CO)_9CO_2$ moieties derived from the carboxylic acid $Co_3(CO)_9C{-}CO_2H$. The picturesque symmetry of some of these systems is exemplified in Fig. 16.

Acknowledgments

Our own efforts in this area have been generously supported by the Natural Sciences and Engineering Research Council of Canada; acknowledgment is also made to the Donors of the Petroleum Research Fund administered by the American Chemical Society. It is a particular pleasure to thank Professors Gérard Jaouen (Ecole Nationale Supérieure de Chimie, Paris) and Jean-Yves Saillard (Université de Rennes) for many valuable discussions over the last few years. We are also grateful to Professors David Curtis (University of Michigan), Tom Fehlner (Notre Dame University, Indiana) and Hubert Wadepohl (Heidelberg, Germany) for kindly providing unpublished data. Finally, M.J.M. thanks the Université de Versailles, France, for a visiting professorship during which time much of this review was written.

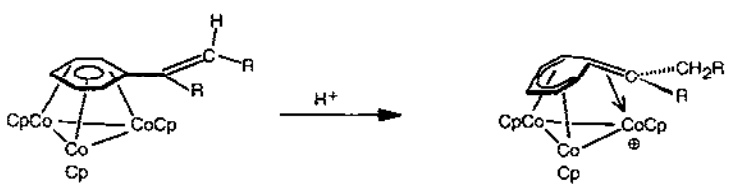

91

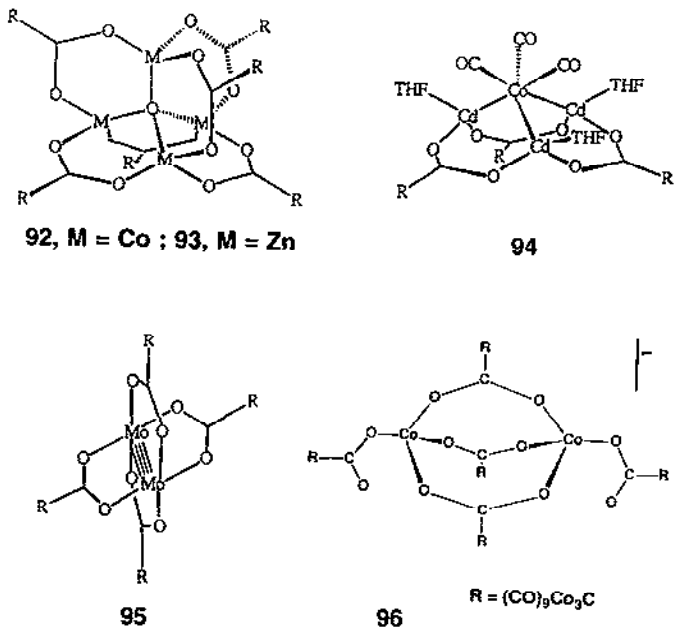

Fig. 16. Inorganometallic clusters coated with peripheral $Co_3(CO)_9C$ substituents.

References

[1] R.T. Morrison and R.N. Boyd, Organic Chemistry, Allyn and Bacon, Boston, 4th edn., 1983, pp. 495–496.
[2] (a) E.A. Hill and R. Wiesner, J. Am. Chem. Soc., 91 (1969) 510. (b) R. Gleiter, R. Seeger, H. Binder, E. Fluck and M. Cais, Angew. Chem., Int. Ed. Engl., 11 (1972) 1028. (c) J.J. Dannenberg, M.K. Levenberg and J.H. Richards, Tetrahedron, 29 (1973) 1575.
[3] R.E. Davis, H.D. Simpson, N. Conte and R. Pettit, J. Am. Chem. Soc., 93 (1971) 6688.
[4] D. Seyferth and J.S. Merola, J. Organomet. Chem., 160 (1978) 275.
[5] M.D. Rausch, E.A. Mintz and D.W. Macomber, J. Org. Chem., 45 (1980) 689.
[6] (a) M. Cais, Organomet. Chem. Rev., 1 (1966) 435. (b) L.W. Haynes and R. Pettit, in G.A. Olah and P.v.R. Schleyer (eds.), Carbonium Ions, Vol. 5, Wiley, New York, 1976, pp. 2049–2133.
[7] J.D. Holmes, D.A.K. Jones and R. Pettit, J. Organomet. Chem., 4 (1965) 324.
[8] (a) M. Acampora, A. Ceccon, M. Dal Farra, G. Giacometti and G. Rigatti, J. Chem. Soc., Perkin Trans., 2 (1977) 483. (b) A. Ceccon, A. Gobbo and A. Venzo, J. Organomet. Chem., 162 (1978) 311.
[9] D. Seyferth, J.S. Merola and J.S. Eschbach, J. Am. Chem. Soc., 100 (1978) 4124.
[10] P.A. Downton, B.G. Sayer and M.J. McGlinchey, Organometallics, 11 (1992) 3281.
[11] K.L. Malisza, L.C.F. Chao, J.F. Britten, B.G. Sayer, G. Jaouen, S. Top, A. Decken and M.J. McGlinchey, Organometallics, 12 (1993) 2462.
[12] S. Lupon, M. Kapon, M. Cais and F.H. Herbstein, Angew. Chem., Int. Ed. Engl., 11 (1972) 1025.
[13] U. Behrens, J. Organomet. Chem., 182 (1979) 89.
[14] T.A. Albright, R. Hoffmann and P. Hoffmann, Chem. Ber., 111 (1978) 1591.
[15] K. Wade, in B.F.G. Johnson (ed.), Transition Metal Clusters, Wiley-Interscience, New York, 1980, pp. 193–264.
[16] D.M.P. Mingos, Acc. Chem. Res., 17 (1984) 331.

[17] M.J. McGlinchey, M. Mlekuz, P. Bougeard, B.G. Sayer, A. Marinetti, J.-Y. Saillard and G. Jaouen, Can. J. Chem., 61 (1983) 1319.
[18] (a) R. Markby, I. Wender, R.A. Friedel, F.A. Cotton and H.W. Sternberg, J. Am. Chem. Soc., 14 (1958) 6529. (b) P.W. Sutton and L.F. Dahl, J. Am. Chem. Soc., 89 (1967) 261.
[19] D. Seyferth, Adv. Organomet. Chem., 14 (1976) 97.
[20] J.E. Hallgren, C.S. Eschbach and D. Seyferth, J. Am. Chem. Soc., 94 (1975) 2547.
[21] J.D. Roberts and M.C. Caserio, Basic Principles of Organic Chemistry, W.A. Benjamin, New York, 1964, pp. 520–521.
[22] R. Ercoli, E. Santambrogio and G. Tettamante Casagrande, Chim. Ind. (Milano), 44 (1962) 1344.
[23] D. Seyferth, G.H. Williams and C.L. Nivert, Inorg. Chem., 16 (1977) 758.
[24] B.E.R. Schilling and R. Hoffmann, J. Am. Chem. Soc., 101 (1979) 3456.
[25] M. Elian and R. Hoffmann, Inorg. Chem., 14 (1975) 1058.
[26] J.W. Kolis, E.M. Holt and D.F. Shriver, J. Am. Chem. Soc., 105 (1983) 7307.
[27] J.W. Kolis, E.M. Holt, J.R. Hriljac and D.F. Shriver, Organometallics, 3 (1984) 496.
[28] M.J. Sailor and D.F. Shriver, Organometallics, 4 (1985) 1476.
[29] A.M. Crespi and D.F. Shriver, Organometallics, 5 (1986) 1750.
[30] M.J. West, M.J. Sailor, P.L. Bogdan, C.P. Brock and D.F. Shriver, J. Am. Chem. Soc., 109 (1987) 6023.
[31] J.R. Shapley, D.S. Strickland, G.M. St. George, M.R. Churchill and C. Bueno, Organometallics, 2 (1983) 185.
[32] M.F. D'Agostino, M. Mlekuz, J.W. Kolis, B.G. Sayer, C.A. Rodger, J.-F. Halet, J.-Y. Saillard and M.J. McGlinchey, Organometallics, 5 (1986) 2345.
[33] E. Delgado, J.C. Jeffery and F.G.A. Stone, J. Chem. Soc., Dalton Trans., (1986) 2105.
[34] (a) W. Bernhardt and H. Vahrenkamp, Angew. Chem., Int. Ed. Engl., 23 (1984) 141. (b) T. Albiez and H. Vahrenkamp, Angew. Chem., Int. Ed. Engl., 26 (1987) 572, and references cited therein.
[35] R.T. Edidin, J.R. Norton and K. Mislow, Organometallics, 1 (1982) 561.
[36] M.F. D'Agostino, C.S. Frampton and M.J. McGlinchey, J. Organomet. Chem., 394 (1990) 145.
[37] M.F. D'Agostino, M. Mlekuz and M.J. McGlinchey, J. Organomet. Chem., 345 (1988) 371.
[38] R.W. Rudolph, Acc. Chem. Res., 9 (1976) 446.
[39] R. Hoffmann, Angew. Chem., Int. Ed. Engl., 21 (1982) 711, and references cited therein.
[40] K.M. Nicholas and R. Pettit, J. Organomet. Chem., 44 (1972) C21.
[41] R.E. Connor and K.M. Nicholas, J. Organomet. Chem., 125 (1977) C45.
[42] S. Padmanabhan and K.M. Nicholas, J. Organomet. Chem., 212 (1984) C23.
[43] S.L. Schreiber, M.T. Klimas and S. Sammakia, J. Am. Chem. Soc., 109 (1987) 5749.
[44] D. Osella, G. Dutto, G. Jaouen, A. Vessières, P.R. Raithby, L. De Benedetto and M.J. McGlinchey, Organometallics, 12 (1993) 4545.
[45] V.I. Solokov, I.V. Barinov and O.A. Reutov, Izv. Akad. Nauk SSR, Ser. Khim., (1982) 1922.
[46] I.V. Barinov, O.A. Reutov and V.I. Sokolov, Zh. Org. Khim., 22 (1986) 2457.
[47] S.F.T. Froom, M. Green, K.R. Nagle and D.J. Williams, J. Chem. Soc., Chem. Commun., (1987) 1305.
[48] O.A. Reutov, I.V. Barinov, V.A. Chertkov and V.I. Sokolov, J. Organomet. Chem., 297 (1985) C25.
[49] W.I. Bailey, Jr., M.H. Chisholm, F.A. Cotton and L.A. Rankel, J. Am. Chem. Soc., 100 (1978) 5764.
[50] C. Cordier, M. Gruselle, G. Jaouen, V.I. Bakhmutov, M.V. Galakhov, L.L. Troitskaya and V.I. Sokolov, Organometallics, 10 (1991) 2303.
[51] M.V. Galakhov, V.I. Bakhmutov, I.V. Barinov and O.A. Reutov, J. Organomet. Chem., 421 (1991) 65.
[52] A. Meyer, D.J. McCabe and M.D. Curtis, Organometallics, 6 (1987) 1491.
[53] H. El-Amouri, J. Vaissermann, Y. Besace, K.P.C. Vollhardt and G.E. Ball, Organometallics, 12 (1993) 605.
[54] H. El-Amouri, Y. Besace, J. Vaissermann, G. Jaouen and M.J. McGlinchey, Organometallics, 13 (1994) 4426.
[55] M.V. Galakhov, V.I. Bakhmutov and I.V. Barinov, Magn. Reson. Chem., 29 (1991) 506.
[56] S. Tondu, G. Jaouen, M.F. D'Agostino and K.L. Malisza, Can. J. Chem., 70 (1992) 1743.
[57] I.V. Barinov, O.A. Reutov, A.V. Polyakov, A.L. Yanovsky, Yu.T. Struchkov and V.I. Sokolov, J. Organomet. Chem., 418 (1991) C24.
[58] N. Leberre-Cosquer, R. Kergoat and P. L'Haridon, Organometallics, 11 (1992) 721.

[59] C. Cordier, M. Gruselle, J. Vaissermann, L.L. Troitskaya, V.I. Bakhmutov, V.I. Sokolov and G. Jaouen, Organometallics, 11 (1992) 3825.
[60] M. Gruselle, C. Cordier, M. Salmain, H. El-Amouri, C. Guérin, J. Vaissermann and G. Jaouen, Organometallics, 9 (1990) 2993.
[61] M. Gruselle, H. El Hafa, M. Nikolski, G. Jaouen, J. Vaissermann, L. Li and M.J. McGlinchey, Organometallics, 12 (1993) 4917.
[62] M. Kondratenko, H. El Hafa, M. Gruselle, J. Vaissermann, G. Jaouen and M.J. McGlinchey, J. Am. Chem. Soc., in press.
[63] H.B. Bürgi and J.D. Dunitz, Acc. Chem. Res., 16 (1983) 153.
[64] H.B. Bürgi, J.D. Dunitz and E. Shefter, J. Am. Chem. Soc., 95 (1973) 5065.
[65] J.E. Baldwin, J. Chem. Soc., Chem. Commun., (1976) 734.
[66] E. Bye, W.B. Schweizer and J.D. Dunitz, J. Am. Chem. Soc., 104 (1982) 5893.
[67] D. Gust and K. Mislow, J. Am. Chem. Soc., 95 (1973) 1535.
[68] J.F. Blount, P. Finocchiaro, D. Gust and K. Mislow, J. Am. Chem. Soc., 95 (1973) 7019.
[69] J.D. Andose and K. Mislow, J. Am. Chem. Soc., 96 (1974) 2168.
[70] K. Mislow, Acc. Chem. Res., 9 (1976) 26.
[71] R.H. Crabtree and M. Lavin, Inorg. Chem., 25 (1986) 805.
[72] L. Girard, P.E. Lock, H. El-Amouri and M.J. McGlinchey, J. Organomet. Chem., 478 (1994) 189.
[73] T. Auf der Heyde, Angew. Chem., Int. Ed. Engl., 33 (1994) 823.
[74] D. Seyferth, J.E. Hallgren and C.S. Eschbach, J. Am. Chem. Soc., 96 (1974) 1730.
[75] M. Mlekuz, M.F. D'Agostino, J.W. Kolis and M.J. McGlinchey, J. Organomet. Chem., 303 (1986) 361.
[76] G. Lavigne, in D.F. Shriver, H.D. Kaesz and R.D. Adams (eds.), The Chemistry of Metal Cluster Complexes, VCH, New York, 1990, Chapter 5, pp. 201–302, and references cited therein.
[77] J.R. Hriljac and D.F. Shriver, J. Am. Chem. Soc., 109 (1987) 6010.
[78] D. Seyferth and M.O. Nestle, J. Am. Chem. Soc., 103 (1981) 3320.
[79] R.A. Gates, M.F. D'Agostino, R.E. Perrier, B.G. Sayer and M.J. McGlinchey, Organometallics, 6 (1987) 1181.
[80] G.L. Geoffroy and S.L. Bassner, Adv. Organomet. Chem., 28 (1983) 1–83.
[81] K.M. Nicholas, Acc. Chem. Res., 20 (1986) 207.
[82] S.L. Schreiber, S. Sammakia and W.E. Crowe, J. Am. Chem. Soc., 108 (1986) 3128.
[83] M.F. D'Agostino, C.S. Frampton and M.J. McGlinchey, Organometallics, 9 (1990) 2972.
[84] K.M. Nicholas, M. Mulvaney and M. Bayer, J. Am. Chem. Soc., 102 (1980) 2508.
[85] S. Top and G. Jaouen, J. Org. Chem., 46 (1981) 78.
[86] M. Gruselle, V. Philomin, F. Chaminant, G. Jaouen and K.M. Nicholas, J. Organomet. Chem., 399 (1990) 317.
[87] H. El-Amouri, M. Gruselle, G. Jaouen, J.C. Daran and J. Vaissermann, Inorg. Chem., 29 (1990) 3238.
[88] H. El-Amouri, M. Gruselle, Y. Besace, J. Vaissermann and G. Jaouen, Organometallics, 13 (1994) 2244.
[89] G. Pourcelot, L. Veniard and P. Cadiot, Bull. Soc. Chim. Fr., (1975) 1275.
[90] J.H. Bestmann and R. Dotzer, Synthesis, (1989) 204.
[91] S.C. Bennett, A. Gelling and M.J. Went, J. Organomet. Chem., 439 (1992) 189.
[92] A. Gelling, G.F. Mohmand, J.C. Jeffery and M.J. Went, J. Chem. Soc., Dalton Trans., (1993) 1857.
[93] S.C. Bennett, M.A. Phipps and M.J. Went, J. Chem. Soc., Chem. Commun., (1994) 225.
[94] M.D. McClain, M.S. Hay, M.D. Curtis and J.W. Kampf, Organometallics, 13 (1994) 4377.
[95] J.F. Capon, S. Cornen, N. Leberre-Cosquer, R. Pichon and R. Kergoat, J. Organomet. Chem., 470 (1994) 137.
[96] D.H. Bradley, M.A. Khan and K.M. Nicholas, Organometallics, 8 (1989) 554.
[97] D.H. Bradley, M.A. Khan and K.M. Nicholas, Organometallics, 11 (1992) 2598.
[98] H. El Hafa, C. Cordier, M. Gruselle, Y. Besace, G. Jaouen and M.J. McGlinchey, Organometallics, 13 (1994) 5149.
[99] S. Top, G. Jaouen and M.J. McGlinchey, J. Chem. Soc., Chem. Commun., (1980) 1110.
[100] N.M. Loim, I.A. Mamedyarova, M.N. Nefedova, G.S. Natzke and V.I. Sokolov, Tetrahedron Lett., (1992) 3611.

[101] J.F. King and P. De Mayo, in P. De Mayo (ed.), Molecular Rearrangements, Wiley-Interscience, New York, 1964.
[102] J. Meerwein and K. van Emster, Ber. Dtsch. Chem. Ges., 55 (1922) 2500.
[103] (a) M. Kagawa, Chem. Pharm. Bull., 7 (1959) 306. (b) D.G. Morris, A.G. Shepherd, M.F. Walker and R.W. Jemison, Aust. J. Chem., 35 (1982) 1061.
[104] L.L. Troitskaya, V.I. Sokolov, V.I. Bakhmutov, O.A. Reutov, M. Gruselle, C. Cordier and G. Jaouen, J. Organomet. Chem., 364 (1989) 195.
[105] A.A. Koridze, N.M. Astakhova and P.V. Petrovskii, J. Organomet. Chem., 254 (1983) 345.
[106] G.H. Young, M.V. Raphael, A. Wojcicki, M. Calligaris, G. Nardin and N. Bresciani-Pahor, Organometallics, 10 (1991) 1934.
[107] (a) D.D. Grove, F. Miskevich, C.C. Smith and J.R. Corte, Tetrahedron Lett., (1990) 6277. (b) D.D. Grove, J.R. Corte, R.P. Spencer, M.E. Pauly and N.P. Rath, J. Chem. Soc., Chem. Commun., (1994) 49.
[108] K.L. Malisza, L. Girard, D.W. Hughes, J.F. Britten and M.J. McGlinchey, submitted to Organometallics.
[109] G.G. Melikyan, O. Vostrowsky, W. Bauer, H.J. Bestmann, M. Khan and K.M. Nicholas, J. Org. Chem., 59 (1994) 222.
[110] G. Jaouen, A. Vessières and I.S. Butler, Acc. Chem. Res., 26 (1993) 361.
[111] V.C. Jordan (ed.), Estrogen/Antiestrogen Action and Breast Cancer Therapy, University of Wisconsin Press, Madison, WI, 1986.
[112] G. Jaouen, S. Top, A. Vessières, B.G. Sayer, C.S. Frampton and M.J. McGlinchey, Organometallics, 11 (1992) 4061.
[113] S. Top, G. Jaouen, A. Vessières, J.-P. Abjean, D. Davoust, C.A. Rodger, B.G. Sayer and M.J. McGlinchey, Organometallics, 4 (1985) 2143.
[114] A. Vessières, S. Top, A.A. Ismail, I.S. Butler, M. Louër and G. Jaouen, Biochemistry, 27 (1988) 6659.
[115] S. Top, A. Vessières and G. Jaouen, J. Chem. Soc., Chem. Commun., (1994) 453.
[116] A. Vessières, S. Top, D. Osella, J.-P. Mornon and G. Jaouen, Angew. Chem., Int. Ed. Engl., 31 (1992) 753.
[117] K.M. Nicholas and J.S. Siegel, J. Am. Chem. Soc., 107 (1985) 4999.
[118] J.N. Gerlach, R.M. Wing and P.C. Ellgen, Inorg. Chem., 15 (1976) 2959.
[119] R. Victor, J. Organomet. Chem., 127 (1977) C25.
[120] P. Chini, L. Colli and M. Peraldo, Gazz. Chim. Ital., 90 (1960) 1005.
[121] J. Suades, F. Dahan and R. Mathieu, Organometallics, 7 (1988) 47.
[122] G.K.S. Prakash, H. Buchholz, V.P. Reddy, A. de Meijere and G.A. Olah, J. Am. Chem. Soc., 114 (1992) 1097.
[123] J.B. Lambert, S. Zhang and S.M. Ciro, Organometallics, 13 (1994) 2430.
[124] C.A. Reed, Z. Xie, R. Bau and A. Benesi, Science, 262 (1993) 402.
[125] P.D. Lickiss, Chem. Soc. Rev., (1992) 271.
[126] R. Ruffolo, A. Decken, L. Girard, H.K. Gupta, M.A. Brook and M.J. McGlinchey, Organometallics, 13 (1994) 4328.
[127] S.H. Strauss, Chem. Rev., 93 (1993) 927.
[128] B.F.G. Johnson, J. Organomet. Chem., 475 (1994) 31.
[129] H. Wadepohl, Angew. Chem., Int. Ed. Engl., 31 (1992) 247.
[130] R.L. Sturgeon, M.M. Olmstead and N.E. Schore, Organometallics, 10 (1991) 1649.
[131] W. Cen, K.J. Haller and T.P. Fehlner, Inorg. Chem., 30 (1991) 3120.
[132] W. Cen, K.J. Haller and T.P. Fehlner, Organometallics, 11 (1992) 3499.
[133] W. Cen, P. Lindenfeld and T.P. Fehlner, J. Am. Chem. Soc., 114 (1992) 5451.
[134] T.P. Fehlner, personal communication, 1994.